AD_____
(Leave blank)

Award Number: W81XWH-11-1-0106

TITLE: "Molecular Mechanisms Underlying Genomic Instability in Brca-Deficient Cells."

PRINCIPAL INVESTIGATOR: Dr. Andre Nussenzweig

CONTRACTING ORGANIZATION: The Geneva Foundation

Tacoma, WA 98402

REPORT DATE: March 2012

TYPE OF REPORT: Revised Annual

PREPARED FOR: U.S. Army Medical Research and Materiel Command
Fort Detrick, Maryland 21702-5012

DISTRIBUTION STATEMENT: (Check one)

□X Approved for public release; distribution unlimited

□ Distribution limited to U.S. Government agencies only;
report contains proprietary information

REPORT DOCUMENTATION PAGE

Form Approved
OMB No. 0704-0188

1. REPORT DATE *(DD-MM-YYYY)*	**2. REPORT TYPE**	**3. DATES COVERED** *(From - To)*
March-2012	Revised Annual	1 March 2011–28 February 2012

4. TITLE AND SUBTITLE
"Molecular Mechanisms Underlying Genomic Instability in Brca-Deficient Cells."

5a. CONTRACT NUMBER

5b. GRANT NUMBER
W81XWH-11-1-0106

5c. PROGRAM ELEMENT NUMBER

6. AUTHOR(S)
Dr. Andre Nussenzweig—Principal Investigator

5d. PROJECT NUMBER

5e. TASK NUMBER

5f. WORK UNIT NUMBER

7. PERFORMING ORGANIZATION NAME(S) AND ADDRESS(ES)
The Geneva Foundation
Tacoma, WA 98402

8. PERFORMING ORGANIZATION REPORT NUMBER

9. SPONSORING / MONITORING AGENCY NAME(S) AND ADDRESS(ES)
U.S. Army Medical Research
And Material Command
Fort Detrick, MD 21702-5012

10. SPONSOR/MONITOR'S ACRONYM(S)

11. SPONSOR/MONITOR'S REPORT NUMBER(S)

12. DISTRIBUTION / AVAILABILITY STATEMENT
Approved for public release; distribution unlimited

13. SUPPLEMENTARY NOTES

14. ABSTRACT
Our proposal is to explore the novel notion that it may be possible to restore near normal HR activity in Brca1 cells and tissues. We believe that this phenomenon will lead to targeted therapies to reduce lifetime risk of tumor formation in BRCA1 and potentially BRCA2 carriers.

15. SUBJECT TERMS
BRCA1, 53BP1, cancer biology, DNA repair, tumorigenesis.

16. SECURITY CLASSIFICATION OF:			**17. LIMITATION OF ABSTRACT**	**18. NUMBER OF PAGES**	**19a. NAME OF RESPONSIBLE PERSON**
a. REPORT	**b. ABSTRACT**	**c. THIS PAGE**			**19b. TELEPHONE NUMBER** *(include area code)*
U	U	U	UU	33	

Standard Form 298 (Rev. 8-98)
Prescribed by ANSI Std. Z39.18

Table of Contents

Page

Introduction

Genomic instability is a hallmark of cancer. Central to a cell's ability to maintain genomic stability are systems that monitor and repair DNA double strand breaks (DSBs). The objective of this study is to understand how the choice of pathways used to repair DNA damage determines whether the repair is error free or causes genomic instability. In mammalian cells, homologous recombination (HR) and nonhomologous end joining (NHEJ) are the two major pathways involved in the repair of DNA DSBs. The Brca1 gene is required for DNA repair by homologous recombination and normal embryonic development. Additionally, protein 53BP1 promotes ligation and facilitates end joining. In previous studies, we have demonstrated that Brca1 and 53BP1 can compete for the processing of DSBs and that 53BP1 can promote genomic instability in the absence of Brca1. Thus, the tumor suppressive function of Brca1 does not appear to be absolute and can be modulated by altering the ability of cells to carryout NHEJ. Our study focuses on shifting the balance between these two repair pathways (HR and NHEJ) to restore error free repair and genomic stability. We believe that a better understanding of mechanisms of DSB repair pathway choice may have important therapeutic implications for prevention or treatment of Brca1/2 germline mutation-associated cancers.

Body

Aim 1: Determine the capacity of NHEJ deficiency to rescue defects in homologous recombination (HR). Using various established mouse models where there is a clearly described defect in HR, we will test the role of the NHEJ proteins 53BP1 and Ku in subverting HR.

Task 1: Determine whether deletion of 53BP1 can rescue the embryonic lethality and restore HR activity of a complete Brca1 deletion. Our previous study demonstrated 53BP1 rescue of the hypomorphic Δ11/ Δ11 mouse.

We have now determined that a similar rescue can be observed in the complete absence of all Brca1 activity. This work was recently published (Bunting SF, Callen E et al, Molecular Cell 2011). The relevant data is shown in Table 1 of this publication as follows:

Table 1. Impact of Deletion of Ku or 53BP1 on the Survival of $Brca1^{\Delta11/\Delta11}$ and Brca1-Null Embryos

$Brca1^{\Delta11/+}Ku80^{+/-}$ × $Brca1^{\Delta11/+}Ku80^{+/-}$ Intercross:					
		$Brca1^{\Delta11/\Delta11}Ku80^{+/+}$ or $Brca1^{\Delta11/\Delta11}Ku80^{+/-}$	$Brca1^{+/+}Ku80^{-/-}$ or $Brca1^{\Delta11/+}Ku80^{-/-}$	$Brca1^{\Delta11/\Delta11}Ku80^{-/-}$	Other Genotypes
E13.5 embryos	Expected:	9	9	3	27
(48 screened)	Observed:	4	12	0	32
Live pups	Expected:	30	30	10	90
(160 screened)	Observed:	0	13	0	147
$Brca1^{+/-}$ $53BP1^{+/-}$ × $Brca1^{+/-}$ $53BP1^{+/-}$ Intercross:					
		$Brca1^{-/-}$ $53BP1^{+/+}$ or $Brca1^{-/-}$ $53BP1^{+/-}$	$Brca1^{+/+}$ $53BP1^{-/-}$ or $Brca1^{+/-}$ $53BP1^{-/-}$	$Brca1^{-/-}$ $53BP1^{-/-}$	Other Genotypes
Live pups	Expected:	21.75	21.75	7.25	65.25
(116 screened)	Observed:	0	22	4	90
$Brca1^{+/-}$ $53BP1^{-/-}$ × $Brca1^{+/-}$ $53BP1^{-/-}$ Intercross:					
		$Brca1^{-/-}$ $53BP1^{+/+}$ or $Brca1^{-/-}$ $53BP1^{+/-}$	$Brca1^{+/+}$ $53BP1^{-/-}$ or $Brca1^{+/-}$ $53BP1^{-/-}$	$Brca1^{-/-}$ $53BP1^{-/-}$	Other Genotypes
Live pups	Expected:	0	66	22	0
(88 screened)	Observed:	0	72	16	0

Frequency of embryos at day E13.5 and live-born pups of the indicated genotypes is shown. See also Table S1.

Task 2: Cross mice containing floxed alleles of Brca1, Brca2, PALB2, and BLM with 53BP1$^{+/-}$ mice to generate animals containing floxed alleles of the various HR factors and either 53BP1$^{+/+}$ or 53BP1$^{-/-}$ status (to produce, for example,. Brca2$^{f/f}$53BP1$^{+/+}$ and Brca2$^{f/f}$53BP1$^{-/-}$).

Task 3: Isolate B cells from the mice bred in this way and infect ex vivo with retroviral Cre recombinase to generate single or doubly deficient cells (e.g. Brca2 deficient B cells with and without 53BP1). We proposed to test these cells for HR reconstitution by assaying for the formation of chromosomal breaks and radial structures, Rad51 foci formation, RPA phosphorylation and PARPi sensitivity.

Tasks 2 and 3 are partially complete. Brca1fl/fl,53BP1-/- and Brca2fl/fl,53BP1-/- mice have been bred and characterized. Data acquired from this project was included in Bunting, Callen et al, Mol Cell 2012, specifically Figure S2A, where we show drug sensitivity of Brca1 knockout cells with and without 53BP1 following Cre-mediated deletion of a Brca1 conditional (floxed) allele:

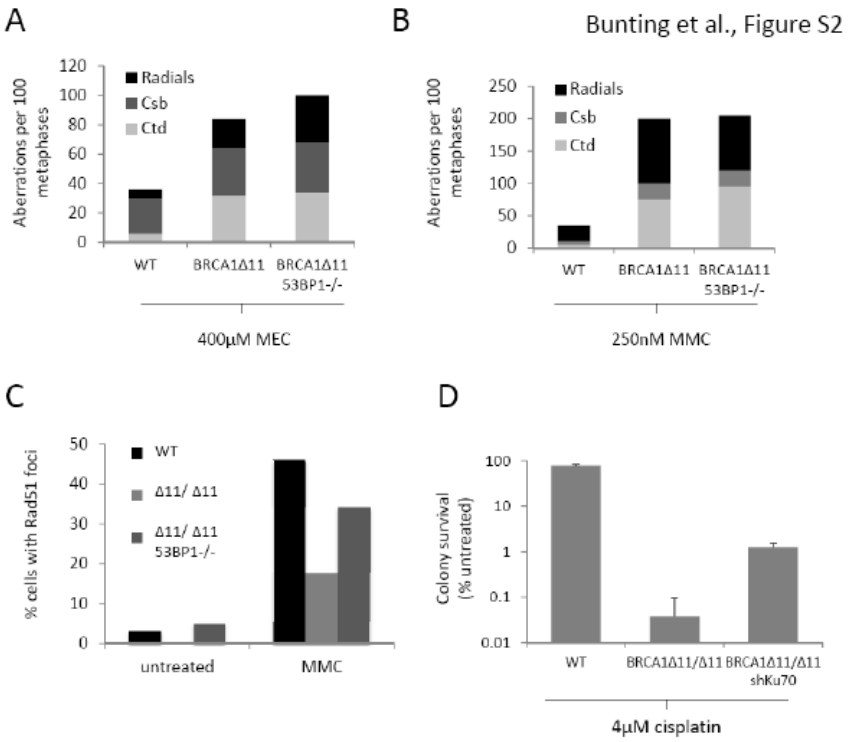

Figure S2, Related to Figure 2.

(A) Quantification of genomic instability in metaphase spreads from WT, *Brca1*$^{\Delta 11/\Delta 11}$ and *Brca1*$^{\Delta 11/\Delta 11}$*53BP1*$^{-/-}$ B cells, treated overnight with 400μM mechlorethamine (MEC). *Brca1*$^{\Delta 11/\Delta 11}$ cells were generated by deletion of a conditional *Brca1*-exon11$^{f/fl}$ allele by Cre recombinase expressed from a *CD19-Cre* knock-in allele.

The PALB2fl/fl x 53BP1 and Blmfl/fl x 53BP1 crosses have given mice of the required genotype but these mice have not yet been characterized.

Task 5: Perform similar analyses as in Task 2 and 3 by crossing FANCD2$^{-/-}$ (that are viable) with 53BP1$^{+/-}$ mice to generate single and doubly deficient B cells (FANCD2$^{-/-}$53BP1$^{+/+}$ and FANCD2$^{-/-}$53BP1$^{-/-}$).

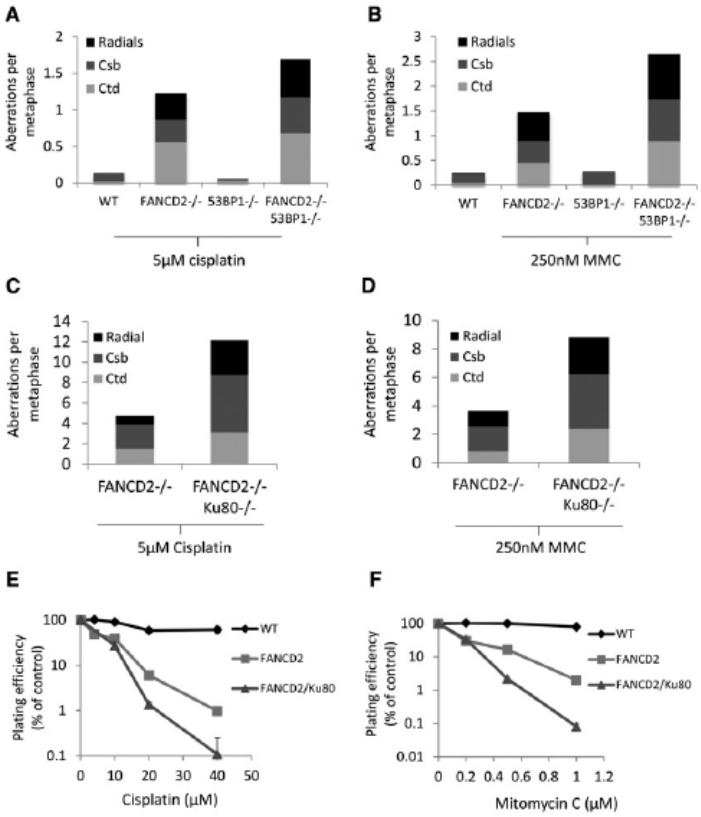

CD-deficient phenotypes. This data 2012:

Figure 5. Genomic Instability in Metaphases from Cells Treated Overnight with Drugs to Induce DNA Interstrand Crosslinks

(A) Genomic instability in B cells from WT, *FANCD2*$^{-/-}$, and *FANCD2*$^{-/-}$*53BP1*$^{-/-}$ mice treated overnight with 5 μM cisplatin.

(B) Genomic instability in B cells from WT, *FANCD2*$^{-/-}$, and *FANCD2*$^{-/-}$*53BP1*$^{-/-}$ mice treated overnight with 250 nM mitomyin C (MMC).

(C) Total genomic aberrations in metaphases from *FANCD2*$^{-/-}$ and *FANCD2*$^{-/-}$*Ku80*$^{-/-}$ mouse embryonic fibroblast cells after overnight treatment with 5 μM cisplatin.

(D) Genomic instability in metaphases from *FANCD2*$^{-/-}$ and *FANCD2*$^{-/-}$*Ku80*$^{-/-}$ after overnight treatment with 250 nM MMC.

(E) Colony forming assay in WT, *FANCD2*$^{-/-}$, and *FANCD2*$^{-/-}$*Ku80*$^{-/-}$ MEFs treated with cisplatin.

(F) Colony forming assay WT, *FANCD2*$^{-/-}$, and *FANCD2,Ku80* double knockout MEFs treated with mitomycin C. (Mean ± standard deviation shown.) See also Figure S5.

Task 6: Tests whether embryonic lethality in mice lacking any of the Brca2, PALB2, FANCD2, or BLM genes could be overcome by combined knockout of the 53BP1 gene. Rates of breast cancer will be compared in 53BP1-sufficient and -deficient mice in which HR genes are deleted in mammary tissue using the Cre transgene under the control of the MMTV LTR promoter.

This task is partially complete. For Brca2, we will not attempt to rescue embryonic lethality by crossing the constitutive knockout to 53BP1. There was no indication from crossing 53BP1-/- to Brca2fl/fl mice that 53BP1 deletion rescued the defect in homologous recombination in the Brca2-deficient background, as shown by the following unpublished data:

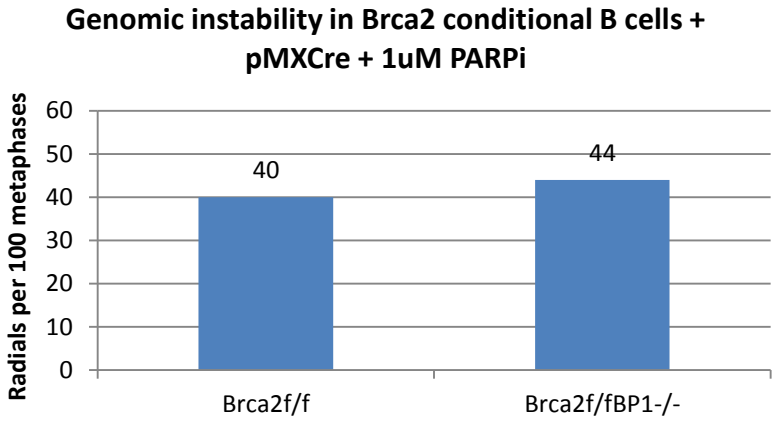

For PALB2 and Blm, we still have to characterize the effect of 53BP1 deletion on the conditional mice so we have not started crossing to the constitutive nulls as yet.

Task 7: Tests if deletion of the Ku70/Ku80 genes can, as was previously demonstrated for 53BP1, rescue the embryonic lethality of Brca1$^{\Delta 11/\Delta 11}$ mice. If successful, MEFs and B cells were to be derived from the offspring and cellular HR activity would be assessed as described in Task 3. If Ku deficiency did not rescue Brca1$^{\Delta 11/\ \Delta 11}$ mice we planned to 'knockdown' Ku in immortalized Brca1$^{\Delta 11/\ \Delta 11}$ or Brca1$^{\Delta 11/\ \Delta 11}$53BP1$^{-/-}$ MEFs to see if we can increase the degree of HR competency.

This task is complete. Ku deletion does not rescue embryonic lethality of Brca1-deficient mice but does afford some rescue of genomic instability in somatic cells with absence of Brca1 activity. This was published in Bunting, Callen et al, Mol Cell, 2012 as Figure 5, shown above in this report (see section for 'Task 5').

Aim 2: Determine the domain of 53BP1 that inhibits HR in Brca1-deficient mice. We will use a combined in vitro and in vivo reconstitution approach to define the functional domains of 53BP1 that regulate the observed HR defects seen in Brca1-deficient cells.

Task 1: Use an *in vivo* genetic approach with recently generated 53BP1 knockin mice to determine the domain of 53BP1 regulating HR activity. Through an established collaboration (M. Nussenzweig, Rockefeller Univ) we currently have four separate 53BP1 knockin mice carrying a deletion of the BRCT domain 53BP1^{DB}, an inactivating mutation in the Tudor domain 53BP1^{DR}, a deletion of the H2AX binding domain 53BP1^{DX} and a combined Tudor and H2AX binding domain mutant, 53BP1^{DXDR}. These mice are unpublished reagents. We plan to cross four unpublished 53BP1 knockin mice with our Brca1$^{\Delta 11/\Delta 11}$ mice and assess whether they can recapitulate the phenotypic rescue observed in the complete null 53BP1$^{-/-}$ mice.

This task is complete. The mouse crosses gave results in line with the retroviral complementation approach described in Aim2, Task 2 (see below for data). We decided that further aging the mice would not reveal new biology.

Task 2: Complement and extend the approach in the above task using reconstitution of 53BP1 mutants into Brca1$^{\Delta 11/\Delta 11}$53BP1$^{-/-}$ B cells. We will use retroviral gene transfer to transduce these B cells with various structural mutants of 53BP1. Given that Brca1$^{\Delta 11/\Delta 11}$53BP1$^{-/-}$ B cells are resistant to PARP inhibitors, we will use restoration of PARP sensitivity as an initial screen to determine the relevant domain of 53BP1 required for inhibiting HR activity. Retroviral constructs will include full length 53BP1, 53BP1^{DB}, 53BP1^{DR}, 53BP1^{DX} and 53BP1^{DXDR} as well as retroviruses encoding the minimal foci formation domain (amino acid 1036-1695) of 53BP1 and the less well characterized N-terminal half of 53BP1 extending through the oligomerization domain (amino acids 1216-1255).

This task is complete and resulted in a senior authorship paper for the awardee, Dr Andre Nussenzweig (Bothmer A, Robbiani D et al, Molecular Cell, 2011). The relevant data was shown in Figure 7 of that paper as:

A

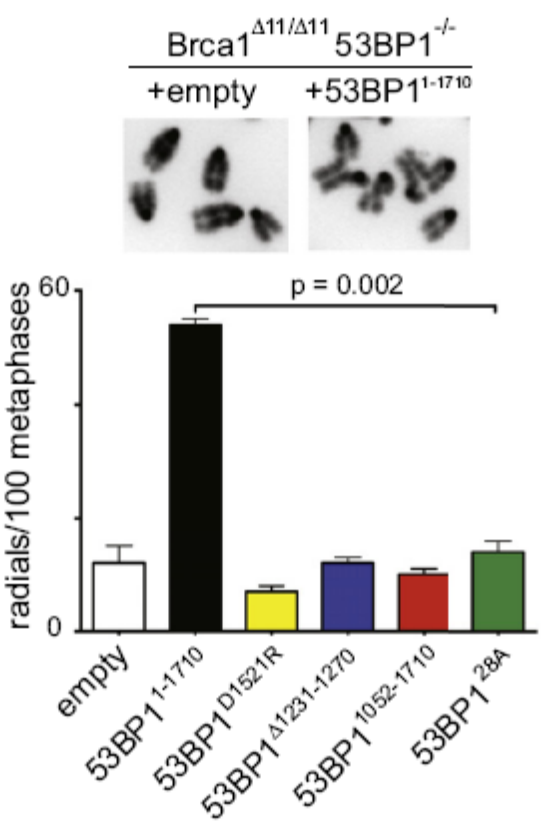

B

Domains of 53BP1	IRIF	Chromatin binding	CSR	Resection
BRCT	D	D	D	D
Tudor (D1518/D1521)	R	R	R	R
Oligomerization	R	D	R	R
N-terminal Phosphorylations	D	D	R	R

D = dispensable R = required

Figure 7. Domains of 53BP1 Required for Preventing DNA End Resection

(A) Brca1$^{\Delta 11/\Delta 11}$53BP1$^{-/-}$ B cells reconstituted with 53BP1 mutant retroviruses. Top: Examples of normal metaphases (+empty) or metaphases containing radial chromosome structures (+53BP1$^{1-1710}$). Bottom: Histogram quantitating the number of radial structures upon infection with the indicated retroviruses. Error bars indicate standard error of the mean. Two independent experiments.

(B) Table summarizing which functional domains of 53BP1 are required (R) or dispensable (D) for IRIF, chromatin binding, CSR, and protection of DNA ends from resection.

See also Figure S6.

Aim 3: Develop small molecule inhibitors of 53BP1 as possible lead compounds to inhibit Brca-mediated tumor formation. This highly ambitious project is ongoing.

Task 1: Construct a GFP-53BP1 expression vector containing the minimal foci forming domain of 53BP1 and create stable cell line that has robust inducible foci formation following DNA damage (adriamycin treatment).

We have determined conditions for measuring 53BP1 foci using an alternative immunofluorescence approach that gives robust foci following treatment with the radiomimetic drug, neocarzinostatin (NCS). In collaboration with Dr. Ty Voss of the High-Throughput Microscopy Core at NIH, we have been able to visualize the foci using the automated Perkin-Elmer Opera platform that will enable screening of the NCI Diversity Set by measuring the suppression of the appearance of 53BP1 foci by any potential lead compound. Currently we are optimizing this system with appropriate positive and negative controls. This work will enable us to conduct a screen of the NIH Diversity Set of small molecules, thereby enabling us to carry out the more detailed screening approaches entailed in Tasks 2-6 of Specific Aim 3.

Key Research Accomplishments

- Deletion of the DNA damage response gene, 53BP1, allows survival of BRCA1-nullizygous mice
- Genomic instability and hypersensitivity of BRCA1-deficient cells to inhibitors of polyADP-ribose polymerase (PARP inhibitors, PARPi) is suppressed by deletion of 53BP1.
- 53BP1 deletion does not rescue genomic instability in BRCA2-null cells.
- Association of 53BP1 with chromatin through the Tudor domain is essential for the role of 53BP1 in promoting genomic instability in BRCA1-deficient cells
- Association of 53BP1 with p53 through the 53BP1 BRCT domain has no impact on the effect of 53BP1 in causing genomic instability in BRCA1-deficient cells.

Reportable Outcomes

1. Two high-impact papers have been published or are in press based on this work with the awardee, Dr. Andre Nussenzweig as senior author (Bothmer, A, Robbiani DF et al, Molecular Cell, 2011 and Bunting SF, Callen E et al, Molecular Cell, 2012).
2. Invited keynote presentation by Dr. Andre Nussenzweig at the international 'Mechanisms of Genomic Instability' meeting in Bahamas, March 2012.
3. Poster presentation by Dr. Elsa Callen at the international 'Mechanisms of Genomic Instability' meeting in Bahamas, March 2012.
4. Several retroviral expression constructs have been generated that provide a new resource for testing molecular function of 53BP1.

Conclusion

This work has revealed for the first time that deletion of 53BP1 prevents genomic instability in cells lacking the tumor suppressor, BRCA1. 53BP1 therefore plays a key role in cellular changes leading to cancer in individuals with BRCA1 mutations. This validates the targeting of 53BP1 as a chemopreventive measure to avert the appearance of cancer in women with mutations in BRCA1, which accounts for ~5%

of all annual cases of breast cancer and a higher proportion of ovarian cancers. This work further suggests that 53BP1 inactivation is a potential pathway leading to resistance of BRCA1-deficient tumors to chemotherapeutic regimens involving PARP inhibitors.

References

Regulation of DNA end joining, resection, and immunoglobulin class switch recombination by 53BP1. Bothmer A, Robbiani DF, Di Virgilio M, Bunting SF, Klein IA, Feldhahn N, Barlow J, Chen HT, Bosque D, Callen E, Nussenzweig A*, Nussenzweig MC* *Molecular Cell*, 2011 May 6;42(3):319-29.
* Joint senior authorship.

BRCA1 Functions Independently of Homologous Recombination in DNA Interstrand Crosslink Repair. Bunting SF*, Callen E*, Kozak ML, Kim JM, Wong N, Lopez-Contreras AJ, Ludwig T, Baer R, Faryabi RB, Malhowski A, Chen H, Fernandez-Capetillo O, D'Andrea A, Nussenzweig A. BRCA1 functions independently of homologous recombination in DNA interstrand cross-link repair. *Molecular Cell.* 2012 Apr 27;46(2):125-35.
* Joint first authorship.

Appendices

1. **Regulation of DNA end joining, resection, and immunoglobulin class switch recombination by 53BP1.** Bothmer A, Robbiani DF, Di Virgilio M, Bunting SF, Klein IA, Feldhahn N, Barlow J, Chen HT, Bosque D, Callen E, Nussenzweig A, Nussenzweig MC *Molecular Cell*, 2011 May 6;42(3):319-29.
2. **BRCA1 Functions Independently of Homologous Recombination in DNA Interstrand Crosslink Repair.** Bunting SF, Callen E, Kozak ML, Kim JM, Wong N, Lopez-Contreras AJ, Ludwig T, Baer R, Faryabi RB, Malhowski A, Chen H, Fernandez-Capetillo O, D'Andrea A, Nussenzweig A. BRCA1 functions independently of homologous recombination in DNA interstrand cross-link repair. M*olecular Cell,* 2012 Apr 27;46(2):125-35

Please cite this article in press as: Bunting et al., BRCA1 Functions Independently of Homologous Recombination in DNA Interstrand Crosslink Repair, Molecular Cell (2012), doi:10.1016/j.molcel.2012.02.015

Molecular Cell
Article

BRCA1 Functions Independently of Homologous Recombination in DNA Interstrand Crosslink Repair

Samuel F. Bunting,[1,5] Elsa Callén,[1,5] Marina L. Kozak,[1] Jung Min Kim,[3] Nancy Wong,[1] Andrés J. López-Contreras,[4] Thomas Ludwig,[2] Richard Baer,[2] Robert B. Faryabi,[1] Amy Malhowski,[1] Hua-Tang Chen,[1] Oscar Fernandez-Capetillo,[4] Alan D'Andrea,[3] and André Nussenzweig[1,*]

[1]Laboratory of Genome Integrity, National Cancer Institute, National Institutes of Health, 37 Convent Drive, Room 1108, Bethesda, MD 20892, USA
[2]Institute for Cancer Genetics, Columbia University Medical Center, Irving Cancer Research Center, Room 503A, 1130 Saint Nicholas Avenue, New York, NY 10032, USA
[3]Department of Radiation Oncology, Dana-Farber Cancer Institute, Harvard Medical School, 44 Binney Street, Boston, MA 02115, USA
[4]Genomic Instability Group, Spanish National Cancer Research Center, Madrid, Spain
[5]These authors contributed equally to this work
*Correspondence: andre_nussenzweig@nih.gov
DOI 10.1016/j.molcel.2012.02.015

SUMMARY

Brca1 **is required for DNA repair by homologous recombination (HR) and normal embryonic development. Here we report that deletion of the DNA damage response factor 53BP1 overcomes embryonic lethality in *Brca1*-nullizygous mice and rescues HR deficiency, as measured by hypersensitivity to polyADP-ribose polymerase (PARP) inhibition. However, *Brca1,53BP1* double-deficient cells are hypersensitive to DNA interstrand crosslinks (ICLs), indicating that BRCA1 has an additional role in DNA crosslink repair that is distinct from HR. Disruption of the nonhomologous end-joining (NHEJ) factor, Ku, promotes DNA repair in *Brca1*-deficient cells; however deletion of either *Ku* or *53BP1* exacerbates genomic instability in cells lacking *FANCD2*, a mediator of the Fanconi anemia pathway for ICL repair. BRCA1 therefore has two separate roles in ICL repair that can be modulated by manipulating NHEJ, whereas FANCD2 provides a key activity that cannot be bypassed by ablation of 53BP1 or Ku.**

INTRODUCTION

In mammalian cells, homologous recombination (HR) and nonhomologous end joining (NHEJ) are the two major pathways involved in the repair of DNA double-strand breaks (DSBs) (Kass and Jasin, 2010). HR is initiated by DNA end resection, which involves the production of recombinogenic 3′ single-stranded DNA by the action of several proteins, including BRCA1, Mre11, CtIP, Exo1, and Blm (Gravel et al., 2008; Sartori et al., 2007; Stracker and Petrini, 2011; Yun and Hiom, 2009). Following end resection, single-stranded DNA is stabilized by binding of replication protein A (RPA). Rad51 subsequently replaces RPA on single-stranded DNA, enabling strand invasion at an intact homologous DNA region, which is used as a template for repair (Kass and Jasin, 2010). In contrast to HR, NHEJ directly religates broken DNA. This process is initiated by the Ku70/Ku80 (Ku) heterodimer which binds directly to the break and recruits the catalytic subunit of the DNA-dependent protein kinase (DNA-PKcs), stabilizing and aligning the ends (Getts and Stamato, 1994; Rathmell and Chu, 1994; Taccioli et al., 1994). End rejoining is then completed by activities of the XRCC4/DNA ligase IV (Lig4) complex (Critchlow and Jackson, 1998).

The importance of double-strand break repair in mammalian cells is demonstrated by the tumor predisposition in humans and mice associated with mutation of the HR gene, *Brca1*. Rescue of homologous recombination in *Brca1*-deficient mice, which can be achieved by deletion of the DNA damage response factor, 53BP1, causes a significant reduction in genomic instability and tumor incidence (Bouwman et al., 2010; Bunting et al., 2010; Cao et al., 2009). Although 53BP1 is not a core NHEJ component, it is required for V(D)J recombination, class switch recombination, and fusion of uncapped telomeres, all of which are dependent on NHEJ (Difilippantonio et al., 2008; Dimitrova et al., 2008; Manis et al., 2004; Ward et al., 2003). Rescue of homologous recombination in *Brca1*-deficient cells by deletion of 53BP1 correlates with a significant increase in exonuclease-mediated resection of DNA double-strand breaks (Bothmer et al., 2011; Bunting et al., 2010), highlighting the importance of regulation of DNA end resection in determining DSB repair pathway choice.

Besides its essential role in repairing DSBs that occur spontaneously during DNA replication, HR is also important for repair of DSBs that arise during processing of DNA interstrand crosslinks (ICLs) (Kee and D'Andrea, 2010). ICLs, which are produced by the reaction of certain metabolites and drugs with DNA, activate a repair pathway comprising at least 15 gene products. Mutation of any of these genes causes the human disease Fanconi anemia (FA), which is associated with pancytopenia, tumor predisposition, and hypersensitivity to DNA crosslinking agents (Kee and D'Andrea, 2010; Wang et al., 2007). Several recent reports have indicated that genomic instability in FA cells is dependent on the activity of NHEJ factors (Adamo et al., 2010; Pace et al., 2010). For example, it

Please cite this article in press as: Bunting et al., BRCA1 Functions Independently of Homologous Recombination in DNA Interstrand Crosslink Repair, Molecular Cell (2012), doi:10.1016/j.molcel.2012.02.015

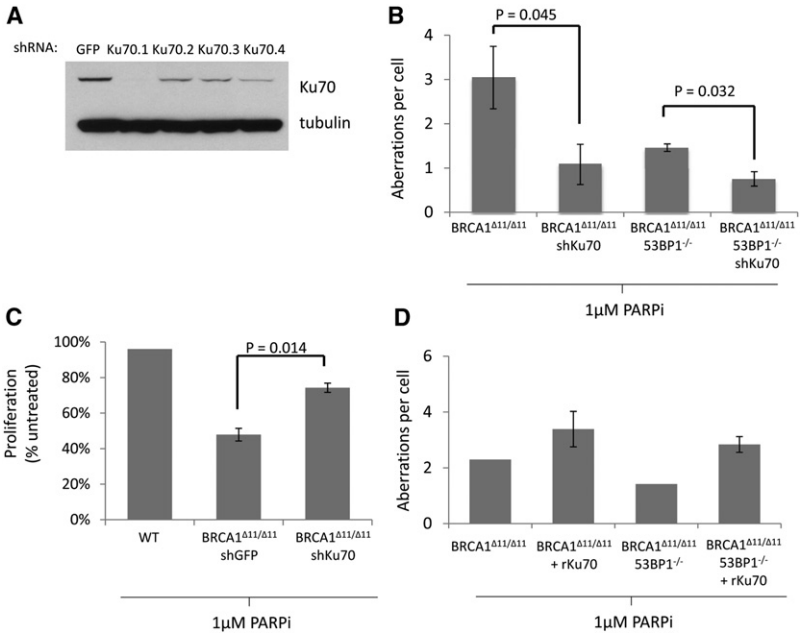

Figure 1. Ku Expression Correlates with Genomic Instability and Reduced Proliferation in *Brca1*-Deficient Cells Treated with PARP Inhibitor

(A) Ku70 expression in cells expressing Ku70 shRNAs. First lane (GFP) shows expression of Ku70 in cells expressing a control shRNA specific for GFP. The GFP and KU70.1 shRNAs were selected for integration into $Brca1^{\Delta11/\Delta11}$ MEFs.

(B) Average genomic instability observed in metaphase spreads from MEF cells treated overnight with 1 μM PARP inhibitor (PARPi).

(C) Proliferation of MEFs growing in the presence of 1 μM PARP inhibitor, relative to untreated cells.

(D) Genomic instability in metaphases from MEFs overexpressing rat Ku70. Error bars show standard deviation in each case. See also Figure S1.

was reported that loss of Ku in *FANCC* mutant chicken or human cells relieved their sensitivity to agents that cause ICLs. Furthermore, the activity of NHEJ has been shown to negatively affect DNA repair in cells lacking the HR factor BRCA2 (Patel et al., 2011).

To gain further insight into how DNA repair involving BRCA1 or factors of the FA pathway is affected by the activity of NHEJ proteins, we have tested the effects of deleting *Ku* or *53BP1* in *Brca1*- and *FANCD2*-deficient mice. Surprisingly, we find that *53BP1* deletion does not affect the sensitivity of *Brca1*-deficient cells to DNA crosslinking agents, despite the previous finding that HR is restored in *Brca1,53BP1* double-deficient cells (Bouwman et al., 2010; Bunting et al., 2010). By contrast, Ku depletion reduces—but does not abrogate—the sensitivity of *Brca1*-deficient cells to both polyADP-ribose polymerase (PARP) inhibitor and cisplatin, suggesting important differences in the roles of Ku70/80 and 53BP1 in response to ICLs. Contrary to the case with *Brca1*-deficient cells, we find that deletion of either *Ku80* or *53BP1* causes an increase in the sensitivity of $FANCD2^{-/-}$ cells to DNA crosslinking drugs. Thus, loss of NHEJ proteins can either cause additive repair defects or suppression of repair defects in response to ICLs.

RESULTS

Genomic Instability and Cell Death in *Brca1*-Deficient Cells after PARP Inhibitor Treatment Is Dependent on Ku and 53BP1

To investigate how Ku contributes to genomic instability in *Brca1*-deficient cells, we knocked down Ku70 in $Brca1^{\Delta11/\Delta11}$ mouse embryonic fibroblasts (MEFs). The $Brca1^{\Delta11}$ allele encodes a mutant isoform of *Brca1* lacking exon 11, which encodes ~50% of the WT protein (Xu et al., 1999b). As we found previously in primary $Brca1^{\Delta11/\Delta11}$ lymphocytes, $Brca1^{\Delta11/\Delta11}$ MEFs are highly sensitive to PARP inhibitor, an agent that is toxic to cells deficient in HR (Bunting et al., 2010) (Figure S1A). We identified a shRNA (Ku70.1) that significantly ablated Ku70 expression in $Brca1^{\Delta11/\Delta11}$ MEFs, as determined by western blotting (Figure 1A). We found that in $Brca1^{\Delta11/\Delta11}$ cells, knockdown of Ku70 caused a significant decrease in the level of genomic instability (chromosome and chromatid breaks, radial chromosomes, and translocations) induced by PARP inhibitor treatment (Figure 1B) and improved proliferation relative to cells expressing a control shRNA (Figure 1C). To further test the importance of Ku70 in modulating the degree of genomic instability in *Brca1*-deficient cells, we prepared cells carrying a stably integrated retroviral construct expressing rat Ku70 (rKu70). Overexpression of Ku70 in these cells led to an increase in genomic instability in $Brca1^{\Delta11/\Delta11}$ and $Brca1^{\Delta11/\Delta11}53BP1^{-/-}$ MEFs (Figures 1D and S1B). Altogether, these results suggest that Ku contributes to genomic instability in $Brca1^{\Delta11/\Delta11}$ cells.

As reported previously, deletion of *53BP1* reduced the level of genomic instability in $Brca1^{\Delta11/\Delta11}$ cells (Figure 1B) and significantly increased the proliferation of these cells in the presence of PARP inhibitor (Figure S1A). Knockdown of Ku70 further reduced the number of chromosome aberrations observed in $Brca1^{\Delta11/\Delta11}53BP1^{-/-}$ cells (Figure 1B), indicating that both Ku70 and 53BP1 contribute to genomic instability in *Brca1*-deficient cells.

$Brca1^{\Delta11/\Delta11}$ and *Brca1*-null mice die in utero (Ludwig et al., 1997; Xu et al., 1999b). However, embryonic lethality in $Brca1^{\Delta11/\Delta11}$ mice can be overcome by additional deletion of *53BP1* (Cao et al., 2009). To test whether deletion of *Ku* could enable an equivalent rescue of embryonic lethality in $Brca1^{\Delta11/\Delta11}$ mice, we bred $Brca1^{\Delta11/+}$ mice to $Ku80^{+/-}$ animals. Whereas we were able to obtain $Brca1^{+/+}Ku80^{-/-}$ and $Brca1^{\Delta11/+}Ku80^{-/-}$ pups, we found that $Brca1^{\Delta11/\Delta11}Ku80^{-/-}$ double-deficient mice did not survive to birth (Table 1). We were also unable to obtain $Brca1^{\Delta11/\Delta11}Ku80^{-/-}$ embryos at E13.5 (Table 1). Thus, in contrast to deletion of *53BP1*, targeting of Ku is not sufficient to overcome the embryonic lethality phenotype seen in $Brca1^{\Delta11/\Delta11}$ mice.

Table 1. Impact of Deletion of Ku or 53BP1 on the Survival of Brca1$^{\Delta11/\Delta11}$ and Brca1-Null Embryos

Brca1$^{\Delta11/+}$ Ku80$^{+/-}$ × Brca1 $^{\Delta11/+}$ Ku80$^{+/-}$ Intercross:					
		Brca1$^{\Delta11/\Delta11}$Ku80$^{+/+}$ or Brca1$^{\Delta11/\Delta11}$Ku80$^{+/-}$	Brca1$^{+/+}$Ku80$^{-/-}$ or Brca1$^{\Delta11/+}$Ku80$^{-/-}$	Brca1$^{\Delta11/\Delta11}$Ku80$^{-/-}$	Other Genotypes
E13.5 embryos	Expected:	9	9	3	27
(48 screened)	Observed:	4	12	0	32
Live pups	Expected:	30	30	10	90
(160 screened)	Observed:	0	13	0	147
Brca1$^{+/-}$ 53BP1$^{+/-}$ × Brca1$^{+/-}$ 53BP1$^{+/-}$ Intercross:					
		Brca1$^{-/-}$ 53BP1$^{+/+}$ or Brca1$^{-/-}$ 53BP1$^{+/-}$	Brca1$^{+/+}$ 53BP1$^{-/-}$ or Brca1$^{+/-}$ 53BP1$^{-/-}$	Brca1$^{-/-}$ 53BP1$^{-/-}$	Other Genotypes
Live pups	Expected:	21.75	21.75	7.25	65.25
(116 screened)	Observed:	0	22	4	90
Brca1$^{+/-}$ 53BP1$^{-/-}$ × Brca1$^{+/-}$ 53BP1$^{-/-}$ Intercross:					
		Brca1$^{-/-}$ 53BP1$^{+/+}$ or Brca1$^{-/-}$ 53BP1$^{+/-}$	Brca1$^{+/+}$ 53BP1$^{-/-}$ or Brca1$^{+/-}$ 53BP1$^{-/-}$	Brca1$^{-/-}$ 53BP1$^{-/-}$	Other Genotypes
Live pups	Expected:	0	66	22	0
(88 screened)	Observed:	0	72	16	0

Frequency of embryos at day E13.5 and live-born pups of the indicated genotypes is shown. See also Table S1.

53BP1 Deletion Does Not Affect the Sensitivity of *Brca1*-Deficient Cells to Cisplatin

Platinum-based drugs such as cisplatin and carboplatin are clinically important agents for the treatment of breast cancer (Cobleigh, 2011). We tested *Brca1*$^{\Delta11/\Delta11}$ and *Brca1*$^{\Delta11/\Delta11}$ *53BP1*$^{-/-}$ cells to determine their sensitivity to cisplatin. Whereas *Brca1*$^{\Delta11/\Delta11}$*53BP1*$^{-/-}$ cells were resistant to PARP inhibitor (Figures 1B and S1A), we found that *Brca1*$^{\Delta11/\Delta11}$ *53BP1*$^{-/-}$ cells were just as sensitive as *Brca1*$^{\Delta11/\Delta11}$ to the effects of cisplatin. This equivalent sensitivity was seen by measurements of both genomic instability in lymphocyte metaphases and colony formation assays using MEFs (Figures 2A and 2B). The high sensitivity of *Brca1*$^{\Delta11/\Delta11}$*53BP1*$^{-/-}$ cells to cisplatin was unexpected, because HR is restored to near WT levels in these cells (Bunting et al., 2010).

Genomic instability in cells treated with cisplatin arises from the ability of cisplatin to form mutagenic intra- and interstrand DNA crosslinks (Kee and D'Andrea, 2010; Wang, 2007). To determine whether intra- or interstrand crosslinks were responsible for cisplatin toxicity in *Brca1*$^{\Delta11/\Delta11}$ and *Brca1*$^{\Delta11/\Delta11}$ *53BP1*$^{-/-}$ cells, we tested two additional agents that produce a high proportion of DNA interstrand crosslinks: nitrogen mustard and mitomycin C (Figures S2A and S2B). *Brca1*$^{\Delta11/\Delta11}$ cells were hypersensitive to both of these drugs, and *53BP1* deletion did not affect sensitivity in either case (Figures S2A and S2B). Thus, even though HR proceeds efficiently, *Brca1*$^{\Delta11/\Delta11}$*53BP1*$^{-/-}$ cells are hypersensitive to a variety of drugs that induce DNA interstrand crosslinks.

The sensitivity of *Brca1*$^{\Delta11/\Delta11}$*53BP1*$^{-/-}$ cells to ICLs indicates that BRCA1 has a function in ICL repair that is separate from its known role in HR. To examine this further, we measured the assembly of nuclear Rad51 foci in cells treated with MMC. Rad51 nucleoprotein assembly is considered to be an essential step in DNA repair by HR (Kass and Jasin, 2010). We observed that, as is the case with ionizing radiation, *Brca1*$^{\Delta11/\Delta11}$ cells showed defective Rad51 foci formation after MMC treatment, but *Brca1*$^{\Delta11/\Delta11}$*53BP1*$^{-/-}$ cells showed Rad51 foci formation at close to wild-type levels (Figure S2C). As *Brca1*$^{\Delta11/\Delta11}$*53BP1*$^{-/-}$ cells are nonetheless highly sensitive to DNA crosslinking agents (Figures 2A and 2B), these data indicate that BRCA1 has a role in DNA crosslink repair that is independent of its previously known role in mediating Rad51 loading at DNA break sites.

Rescue of Embryonic Lethality in *Brca1*-Null Mice by 53BP1 Deletion

To ensure that our results were not specific to cells with the hypomorphic *Brca1*$^{\Delta11}$ allele, we tested the effect of crosslinking drugs in *Brca1*-null cells. *Brca1* nullizygosity has a much more severe phenotype than the *Brca1*$^{\Delta11/\Delta11}$ mutation, with embryonic lethality at E5.5–E8.5 in *Brca1*$^{-/-}$ mice compared to E12.5–E18.5 in *Brca1*$^{\Delta11/\Delta11}$ homozygotes (Ludwig et al., 1997; Xu et al., 1999b). Furthermore, whereas *Brca1*$^{\Delta11/\Delta11}$*p53*$^{+/-}$ animals are viable, embryonic lethality in *Brca1*-null animals cannot be overcome by deletion of *p53* (Xu et al., 2001). Consistent with this, we found that it was not possible to generate *Brca1*$^{-/-}$*53BP1*$^{+/+}$ or *Brca1*$^{-/-}$*53BP1*$^{+/-}$ pups (Table 1). Strikingly, however, double-null *Brca1*$^{-/-}$*53BP1*$^{-/-}$ pups were obtained at a frequency only slightly lower than the expected Mendelian ratio (Table 1). *53BP1* deletion, in contrast to *p53* deletion, is therefore able to rescue embryonic lethality in mice that are null for *Brca1*.

Brca1$^{-/-}$*53BP1*$^{-/-}$ mice appeared normal in all respects except that males were sterile and had small testes (Figure S3A). As was the case with *Brca1*$^{\Delta11/\Delta11}$*53BP1*$^{-/-}$ cells, *Brca1*$^{-/-}$ *53BP1*$^{-/-}$ cells showed resistance to PARP inhibitor (Figure S3B) but were hypersensitive to cisplatin and mitomycin C (Figures S3C– S3F). Hypersensitivity to DNA crosslinking drugs is therefore a common feature of *Brca1*-null and *Brca1*$^{\Delta11/\Delta11}$ cells that cannot be rescued by 53BP1 deletion. Male-specific sterility in *Brca1*$^{-/-}$*53BP1*$^{-/-}$ mice further supports an HR-independent role for BRCA, in this case during spermatogenesis. Female

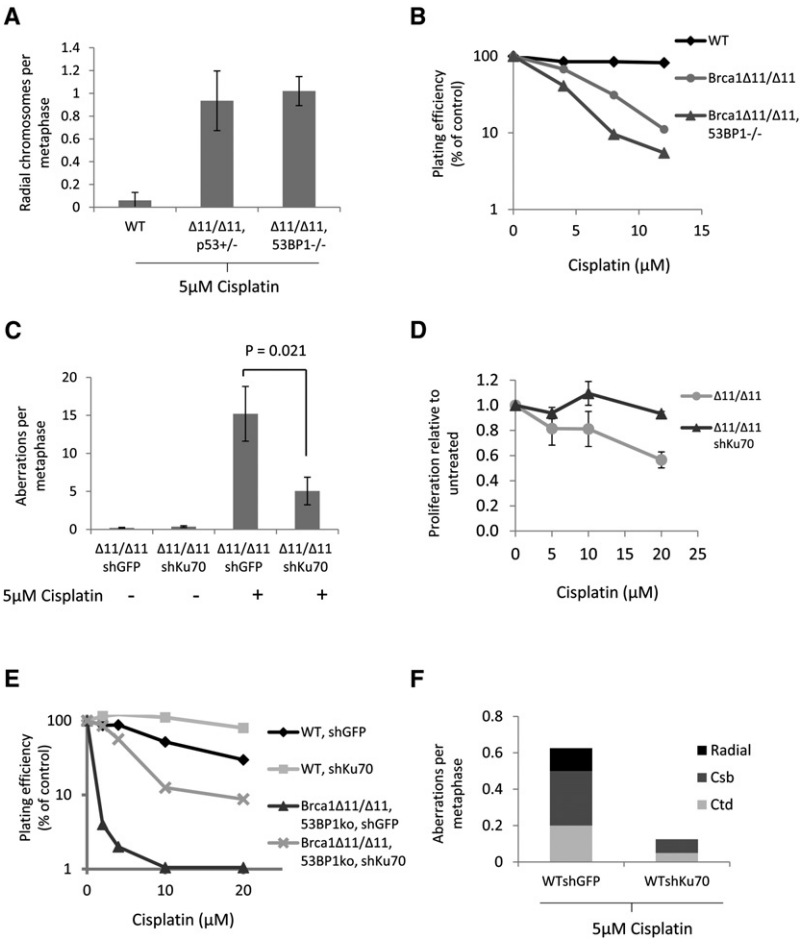

Figure 2. Reduced Genomic Instability and Increased Survival of *Brca1*-Deficient Cells with Ku70 Knockdown after Cisplatin Treatment

(A) Frequency of radial chromosome formation in lymphocytes of the indicated genotypes after overnight treatment with 5 μM cisplatin.

(B) Colony formation in MEFs treated for 2 hr with cisplatin.

(C) Genomic instability in MEFs expressing stably integrated shRNA against either GFP or Ku70, treated overnight with 5 μM cisplatin.

(D) Growth of BRCA1$^{\Delta 11/\Delta 11}$ cells with stably integrated Ku70 shRNA in the presence of cisplatin. Cisplatin was applied for 24 hr and growth assayed with CellTiter-Glo after a total of 5 days.

(E) Colony formation of MEF lines treated for 2 hr with cisplatin.

(F) Genomic instability in control (WTshGFP) or Ku70 knockdown MEFs after overnight treatment with 5 μM cisplatin. Error bars show standard deviation in each case. See also Figure S2.

mice, by contrast, showed normal ovaries and were fertile, suggesting a differential requirement for BRCA1 in male and female gametogenesis. Although *Brca1*-deficient mice were previously shown to have a defect in mammary development (Xu et al., 1999a), we observed no difference in mammary ductal morphogenesis in female WT, *53BP1*$^{-/-}$, or *Brca1*$^{-/-}$*53BP1*$^{-/-}$ mice at pregnancy day P8.5 (Figure S3G).

Cisplatin Cytotoxicity in *Brca1*-Deficient and WT Cells Is Dependent on Ku

As Ku depletion improved the survival of *Brca1*$^{\Delta 11/\Delta 11}$ cells treated with PARP inhibitor (Figure 1C), we tested whether Ku similarly modulated their sensitivity to ICLs. Unlike *53BP1* deletion, we found that Ku70 depletion reduced genomic instability in *Brca1*$^{\Delta 11/\Delta 11}$ MEFs treated with cisplatin and enhanced their proliferative ability in short-term growth assays as well as in long-term clonogenic colony formation assays (Figures 2C, 2D, and S2D). Ku70 depletion was also able to improve the growth of *Brca1*$^{\Delta 11/\Delta 11}$*53BP1*$^{-/-}$ MEFs treated with cisplatin, as measured by colony formation (Figure 2E). Interestingly, we noticed that Ku70 depletion also enabled WT cells to proliferate better after treatment with cisplatin (Figure 2E). This is consistent with a previous report, which showed that deletion of *Ku80* afforded increased survival in WT cells treated with cisplatin (Jensen and Glazer, 2004). Furthermore, improved growth in Ku70-deficient cells after cisplatin treatment correlated with reduced genomic instability (Figure 2F). These findings demonstrate that the presence of Ku sensitizes WT, *Brca1*$^{\Delta 11/\Delta 11}$, and *Brca1*$^{\Delta 11/\Delta 11}$*53BP1*$^{-/-}$ cells to the cytotoxic effects of cisplatin.

Ku Antagonizes HR without Significantly Affecting DSB Resection

Rad51 loading at sites of DNA double-strand breaks is a critical step in repair of DNA damage by HR, and deletion of *53BP1* in *Brca1*-deficient cells was previously shown to increase the proportion of cells with Rad51 foci following DNA damage (Bouwman et al., 2010; Bunting et al., 2010). To address the mechanism by which Ku depletion promotes genome integrity in *Brca1*$^{\Delta 11/\Delta 11}$ cells, we tested whether knockdown of Ku70 could cause an equivalent increase in irradiation-induced Rad51 foci. We found that, although Rad51 foci formation was reduced in *Brca1*$^{\Delta 11/\Delta 11}$ cells relative to WT, knocking down Ku70 caused a statistically significant ($p = 0.0005$) increase in Rad51 foci (Figure 3A), consistent with an increase in DNA repair by HR in the absence of Ku70 (Pierce et al., 2001). An increase in the proportion of irradiated cells exhibiting Rad51 foci after Ku knockdown was also seen in WT and *Brca1*$^{\Delta 11/\Delta 11}$*53BP1*$^{-/-}$ cells, although in these cases the increase did not reach the level of statistical significance.

Exonuclease resection of DNA double-strand breaks is considered to be a critical step in HR, because it generates single-stranded DNA that allows loading of RPA and Rad51 around the break site. To test the extent to which 53BP1 and Ku regulate resection of DNA double-strand breaks, we performed anti-RPA chromatin immunoprecipitation in B cells from WT, *53BP1*$^{-/-}$, and *Ku70*$^{-/-}$ mice. Stimulation of B cells with LPS and IL4 generates multiple DSBs centered around the immunoglobulin heavy chain (IgH) Sμ, Sγ1, Sγ3, and Sε switch regions (Nussenzweig and Nussenzweig, 2010). RPA

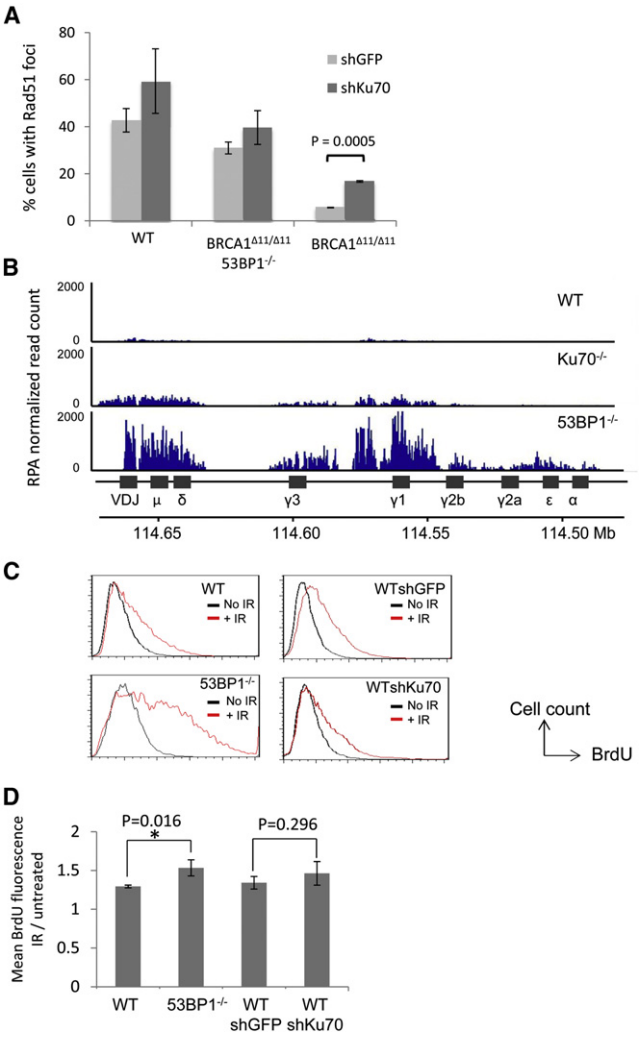

Figure 3. Effect of 53BP1 and Ku on Rad51 Foci and DSB Resection

(A) Quantification of Rad51 immunofluorescence in mouse embryonic fibroblasts of the indicated genotypes. Cells expressing either control shRNA against GFP or shRNA against Ku70 were irradiated (5 Gy, 4 hr recovery) and stained with anti-Rad51 antibody. The average percentages of cells (± standard deviation) with more than 5 nuclear foci from three experiments are shown.

(B) Anti-RPA ChIP-Seq in B cells. B cells were stimulated to undergo class switch recombination in vitro. Chromatin from B cells was harvested 48 hr poststimulation and used for RPA ChIP. RPA read count (normalized by the total library size per million) is shown at the IgH locus.

(C) Nondenaturing anti-BrdU immunofluorescence in MEFs treated with ionizing radiation (30 Gy, 2 hr recovery), measured by flow cytometry. Resection is measured by detection of exposed BrdU (x axis).

(D) Quantification of mean BrdU fluorescence intensity of the irradiated population shown in (C), normalized to the untreated population. Average ± standard deviation from five experiments. See also Figure S4.

loads at the site of DNA double-strand breaks following exonuclease resection, hence a greater enrichment of DNA sequences in the anti-RPA ChIP fraction indicates a greater amount of DSB resection (Yamane et al., 2011). *53BP1*$^{-/-}$ B cells showed a significantly increased extent of pull-down of IgH sequences in the anti-RPA ChIP fraction (Figure 3B), consistent with enhanced resection in these cells. This result is in accordance with previous reports, which suggested that loss of 53BP1 increases the extent of resection of DNA DSBs (Bothmer et al., 2010; Bunting et al., 2010; Difilippantonio et al., 2008). In comparison to *53BP1*$^{-/-}$ cells, however, *Ku70*$^{-/-}$ cells showed only a minor increase in resection relative to WT, as measured by RPA ChIP at IgH (Figure 3B).

To further test the role of NHEJ factors in the regulation of DSB resection, we pulsed WT, *53BP1*$^{-/-}$, and Ku70-depleted MEFs with 5-bromo-2′-deoxyuridine (BrdU) to enable the measurement of single-stranded DNA at ionizing radiation-induced DSBs. We adapted an existing nondenaturing BrdU immunofluorescence protocol for measurement of DSB resection (Sartori et al., 2007) to allow quantification of the amount of resection in a population of cells by flow cytometry (Figure 3C). Notably, we found that *53BP1*$^{-/-}$ cells showed a statistically significant increase in resection after irradiation compared to WT cells (Figures 3C and 3D). In contrast, Ku70-knockdown cells did not significantly increase resection compared to cells expressing a control shRNA. By staining for DNA content in the sample population, we observed that resection was significantly more extensive in cells in the S/G2 phases of the cell cycle (Figure S4A), consistent with previous findings (Huertas, 2010). Taken together, these results indicate that, whereas 53BP1 has a major role in regulating resection of DNA DSBs, Ku plays a more limited role in this process. The increase in Rad51-dependent HR seen in Ku-deficient cells after DNA damage therefore arises from a mechanism other than increased resection (see Discussion).

BRCA1 Mediates FANCD2 Foci Formation after Treatment with Crosslinking Agents

The sensitivity of *Brca1*$^{\Delta11/\Delta11}$*53BP1*$^{-/-}$ cells to DNA crosslinking agents (Figures 2A, 2B, S2A, and S2B) strongly suggests that BRCA1 provides an activity that is required for DNA crosslink repair that is separate from its function in HR. FANCD2 ubiquitylation and recruitment to sites of DNA crosslinks are considered to be essential steps in crosslink repair (Huang and D'Andrea, 2010; Knipscheer et al., 2009; Long et al., 2011). We therefore tested whether these steps are normal in *Brca1*$^{\Delta11/\Delta11}$ and *Brca1*$^{\Delta11/\Delta11}$*53BP1*$^{-/-}$ cells. BRCA1 was previously reported to be dispensable for FANCD2 ubiquitylation, but required for FANCD2 foci formation after DNA damage (Garcia-Higuera et al., 2001; Vandenberg et al., 2003). We found that FANCD2 ubiquitylation, as measured by western blotting, was not significantly altered in either *Brca1*$^{\Delta11/\Delta11}$ or *Brca1*$^{\Delta11/\Delta11}$ *53BP1*$^{-/-}$ cells (Figure 4A). By contrast, the number of cells showing FANCD2 foci after treatment with cisplatin or mitomycin C was reduced in both *Brca1*$^{\Delta11/\Delta11}$ and *Brca1*$^{\Delta11/\Delta11}$*53BP1*$^{-/-}$ cells (Figure 4B). Reduced FANCD2 foci in these cells was not caused by reduced growth rate, as *Brca1*$^{\Delta11/\Delta11}$, *Brca1*$^{\Delta11/\Delta11}$ *53BP1*$^{-/-}$, and WT controls showed a similar cell-cycle distribution (Figure S4B).

We found that depletion of Ku mitigates the toxic effects of DNA crosslinking agents (Figures 2C–2F). We therefore extended our approach by testing whether FANCD2 foci are affected by the presence of Ku70. We found that depletion of Ku70 restored the formation of FANCD2 foci after cisplatin or

Please cite this article in press as: Bunting et al., BRCA1 Functions Independently of Homologous Recombination in DNA Interstrand Crosslink Repair, Molecular Cell (2012), doi:10.1016/j.molcel.2012.02.015

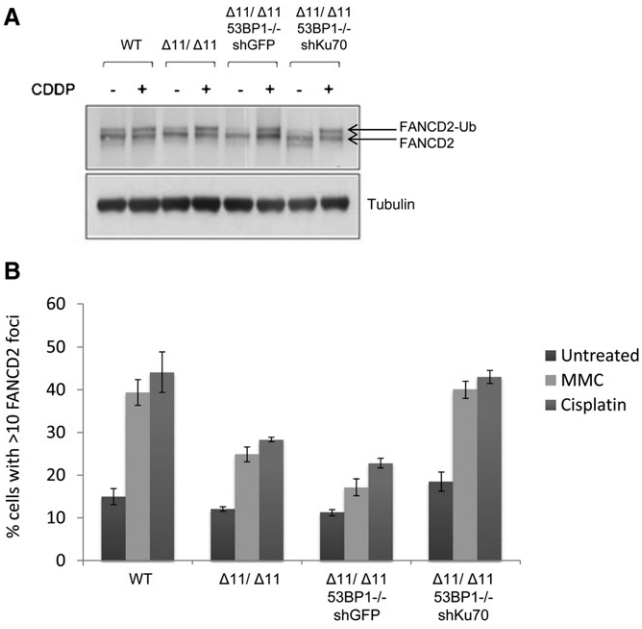

Figure 4. FANCD2 Ubiquitylation and Damage Foci in *Brca1*-Deficient Cells

(A) Western blot showing FANCD2 ubiquitylation in WT, *Brca1*$^{\Delta 11/\Delta 11}$, and *Brca1*$^{\Delta 11/\Delta 11}$*53BP1*$^{-/-}$ MEFs with and without cisplatin (CDDP) treatment. *Brca1*$^{\Delta 11/\Delta 11}$*53BP1*$^{-/-}$ MEFs expressed either control shRNA or shRNA against Ku70.

(B) FANCD2 foci analysis in MEFs treated with either cisplatin or mitomycin C. Cells with more than 10 FANCD2 foci were scored as positive. Mean ± SEM is shown. See also Figure S3.

MMC to a level equivalent to that seen in WT cells (Figure 4B). We conclude that Ku70/80 affects recruitment or retention of FANCD2 at sites of DNA crosslink repair.

Deletion of *53BP1* or *Ku* Exacerbates Genomic Instability in *FANCD2*-Deficient Cells

Hypersensitivity to DNA crosslinking agents is a key diagnostic test for genetic deficiency in components of the Fanconi anemia (FA) pathway (Wang, 2007). Cells from FA patients, or knockout mice with deficiencies in the FA pathway, are unable to repair DNA interstrand crosslinks and tend to accumulate genomic instability with an increased risk of tumorigenesis (Kee and D'Andrea, 2010; Wang, 2007). Recent studies have reported that hypersensitivity of human, nematode, and chicken DT40 cells to interstrand crosslinking agents can be rescued by knockdown, deletion, or inhibition of NHEJ factors such as Ku, Lig4, or DNA-PKcs (Adamo et al., 2010; Pace et al., 2010). To test whether it was possible to prevent genomic instability in FA cells by genetic ablation of DNA damage response factors, we bred mice that were double null for the key FA pathway component, *FANCD2* (Kee and D'Andrea, 2010; Wang, 2007), and either *53BP1* or *Ku80*. Consistent with the reported sensitivity of *FANCD2*$^{-/-}$ cells to DNA crosslinking agents (Houghtaling et al., 2003), cells from *FANCD2*$^{-/-}$ mice were hypersensitive to cisplatin and mitomycin C (Figures 5A and 5B). We found that 53BP1 deletion in *FANCD2*$^{-/-}$ cells led to increased sensitivity to cisplatin (Figure 5A). Similar results were observed with mitomycin C treatment, which induced higher levels of genomic instability in *FANCD2*$^{-/-}$ *53BP1*$^{-/-}$ cells relative to *FANCD2*$^{-/-}$ (Figure 5B). To examine the impact of *53BP1* loss in vivo we examined hematopoietic stem cells (HSCs). *FANCD2*$^{-/-}$ mice have hematopoietic defects, including a 50% reduction in the frequency of both HSCs and common lymphoid progenitors (CLPs) (Zhang et al., 2010). Quantification of HSC and CLP frequencies in double mutant mice revealed that these defects were equivalent in the combined absence of FANCD2 and 53BP1 (Figures S5A and S5B). Thus, loss of 53BP1 renders *FANCD2*-deficient cells more sensitive to DNA crosslinking agents and does not alleviate the severity of hematopoietic defects in mouse models of Fanconi anemia.

Although *Ku80*$^{-/-}$ and *FANCD2*$^{-/-}$ mice are viable, we were not able to obtain live mice that were double null for *FANCD2* and *Ku80* (n = 98 pups screened), suggesting that Ku deficiency also exacerbates developmental defects in the absence of *FANCD2*. This observation is consistent with a previous report, which showed that cells deficient in both *FANCD2* and the NHEJ factor *DNA-PKcs* had a diminished capacity to repair DNA damage compared to either single mutant (Houghtaling et al., 2005). Although we could not obtain double-null pups, we were able to isolate *FANCD2*$^{-/-}$*Ku80*$^{-/-}$ MEFs, and we tested these for their ability to repair interstrand crosslinks induced by cisplatin and mitomycin C. We found that, as compared to *FANCD2*$^{-/-}$ cells, *FANCD2*$^{-/-}$*Ku80*$^{-/-}$ double-knockout MEFs showed increased chromosomal damage in response to either cisplatin (Figure 5C) or mitomycin C (Figure 5D). Colony formation assays with *FANCD2*$^{-/-}$*Ku80*$^{-/-}$ MEFs revealed that these cells grew significantly worse than *FANCD2*$^{-/-}$ single-knockout cells after treatment with cisplatin or mitomycin C (Figures 5E and 5F). These results indicate that FANCD2 provides an essential activity for repair of interstrand crosslinks in murine cells that cannot be rescued by deletion of either *53BP1* or *Ku*. Indeed, the increased severity of the phenotypes observed after combining deficiency in *FANCD2* with loss of either *53BP1* or Ku suggests that NHEJ partially compensates for *FANCD2* deficiency in cisplatin-induced ICL repair.

DISCUSSION

Efficiency of ICL Repair Is Modified by BRCA1 and Ku70/80

Our study reveals that the requirements for BRCA1 in Rad51 nucleoprotein assembly (Bhattacharyya et al., 2000) and FANCD2 retention at DNA damage sites (Vandenberg et al., 2003) represent two distinct activities of the BRCA1 protein. We propose that during ICL repair, BRCA1 functions early at the crosslink excision step and, later, during HR. 53BP1 only affects the function of BRCA1 during the later HR stage. Deletion of 53BP1 therefore has no effect on the hypersensitivity of *Brca1*-deficient cells to agents that cause ICLs. In contrast, Ku affects both steps where BRCA1 is active, hence deletion of Ku reduces the hypersensitivity of *Brca1*-deficient cells to both PARP inhibitors and DNA crosslinking agents. We

Please cite this article in press as: Bunting et al., BRCA1 Functions Independently of Homologous Recombination in DNA Interstrand Crosslink Repair, Molecular Cell (2012), doi:10.1016/j.molcel.2012.02.015

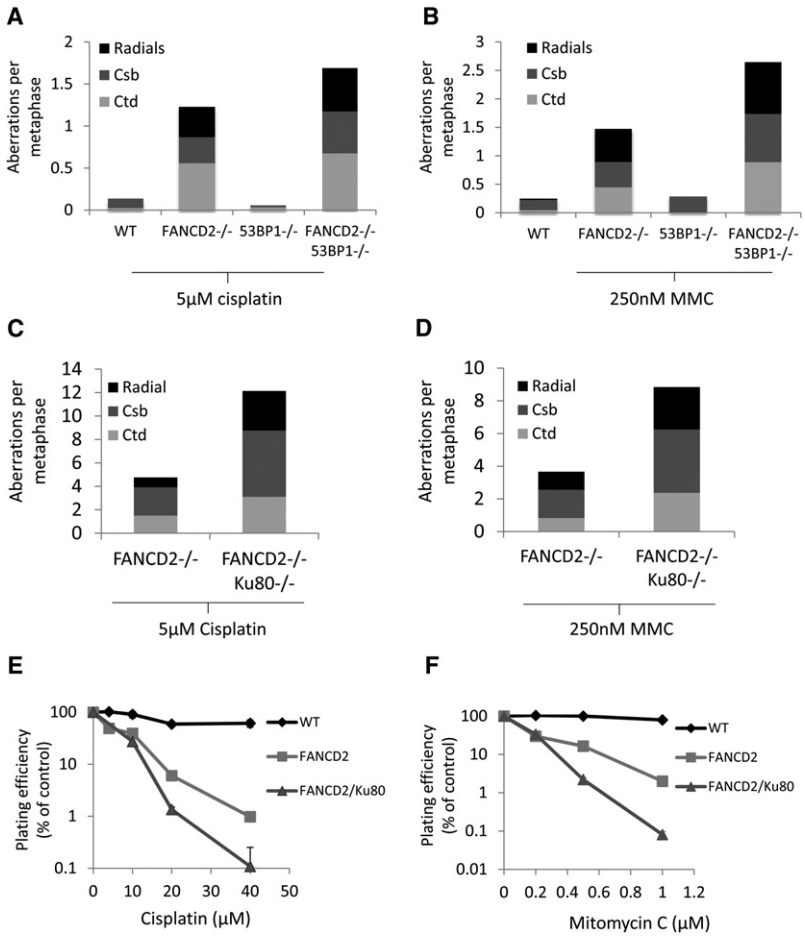

Figure 5. Genomic Instability in Metaphases from Cells Treated Overnight with Drugs to Induce DNA Interstrand Crosslinks

(A) Genomic instability in B cells from WT, *FANCD2*$^{-/-}$, and *FANCD2*$^{-/-}$*53BP1*$^{-/-}$ mice treated overnight with 5 μM cisplatin.

(B) Genomic instability in B cells from WT, *FANCD2*$^{-/-}$, and *FANCD2*$^{-/-}$*53BP1*$^{-/-}$ mice treated overnight with 250 nM mitomyin C (MMC).

(C) Total genomic aberrations in metaphases from *FANCD2*$^{-/-}$ and *FANCD2*$^{-/-}$*Ku80*$^{-/-}$ mouse embryonic fibroblast cells after overnight treatment with 5 μM cisplatin.

(D) Genomic instability in metaphases from *FANCD2*$^{-/-}$ and *FANCD2*$^{-/-}$*Ku80*$^{-/-}$ after overnight treatment with 250 nM MMC.

(E) Colony forming assay in WT, *FANCD2*$^{-/-}$, and *FANCD2*$^{-/-}$*Ku80*$^{-/-}$ MEFs treated with cisplatin.

(F) Colony forming assay WT, *FANCD2*$^{-/-}$, and *FANCD2,Ku80* double knockout MEFs treated with mitomycin C. (Mean ± standard deviation shown.) See also Figure S5.

summarize these results in a model showing the impact of BRCA1 and NHEJ factors in repairing different types of DNA damage (Figure 6).

Increased DSB Resection Associated with *53BP1* Deletion Does Not Improve ICL Repair

Treatment with PARP inhibitor stabilizes single-strand breaks (Figure 6, i), which are converted to double-strand breaks during DNA replication following collapse of the replication fork at a single-strand break (Bryant et al., 2005; Farmer et al., 2005). According to our model, the double-strand break formed by this process can be directed to either HR or NHEJ. The key rate-limiting step is resection of the DSB, which commits repair to HR (Figure 6, ii). *53BP1* deletion significantly increases resection; hence in the absence of 53BP1, error-free HR becomes the principal repair pathway (Figure 6, iii). Cisplatin or MMC treatment produces ICLs. These ICLs cause replication fork collapse, but in this case, the double-strand break is not immediately available for HR, because the homologous template must first be repaired by translesion synthesis (TLS) and nucleotide excision repair (NER) (Figures 6, vii–ix). Increased resection of DSBs mediated by ablation of 53BP1 may not be beneficial to ICL repair and, if so, only at a late stage when TLS and NER are complete. On the other hand, DSBs produced as a consequence of FANCD2-dependent endonuclease action at DNA crosslinks can be inappropriately joined to other DSBs present in the cell by the action of Ku-dependent NHEJ prior to commitment to HR (Figure 6, x). Deletion or knockdown of Ku therefore promotes error-free repair at the sites of ICLs by inhibiting potentially mutagenic repair by NHEJ.

Ku deletion does not rescue the embryonic lethality observed in *Brca1*-deficient mice. This also represents a significant difference compared to deletion of *53BP1*, which rescues the embryonic lethality of homozygous *Brca1*$^{\Delta 11/\Delta 11}$ or *Brca1*-null mice (Table S1) (Bunting et al., 2010). Failure of Ku deletion to rescue the embryonic lethality of *Brca1*-deficient mice correlates with the minor impact on DSB resection that is achieved by targeting Ku relative to *53BP1* (Figures 3B–3D). This difference in DSB resection likely reflects the distinct nature of the interaction between these repair factors and DNA. Whereas Ku binds directly to exposed DNA ends, 53BP1 binds to a histone mark that is present in the entire chromatin area around the double-strand break (Botuyan et al., 2006; Huyen et al., 2004). Any impact that Ku has on resection is therefore likely to be in the immediate vicinity of the DNA end, whereas 53BP1 is capable of impacting resection throughout a much larger chromatin domain. We hypothesize that the ability to bypass the requirement for BRCA1 in mammalian development requires a large extent of recombinogenic single-stranded DNA during replication, which is afforded by *53BP1* deletion, but not by Ku deficiency. In summary, although both Ku and 53BP1 antagonize HR, the impact of these factors in repairing various types of lesions is distinct, because *Ku* promotes mutagenic repair by NHEJ, whereas *53BP1* inhibits DNA end processing.

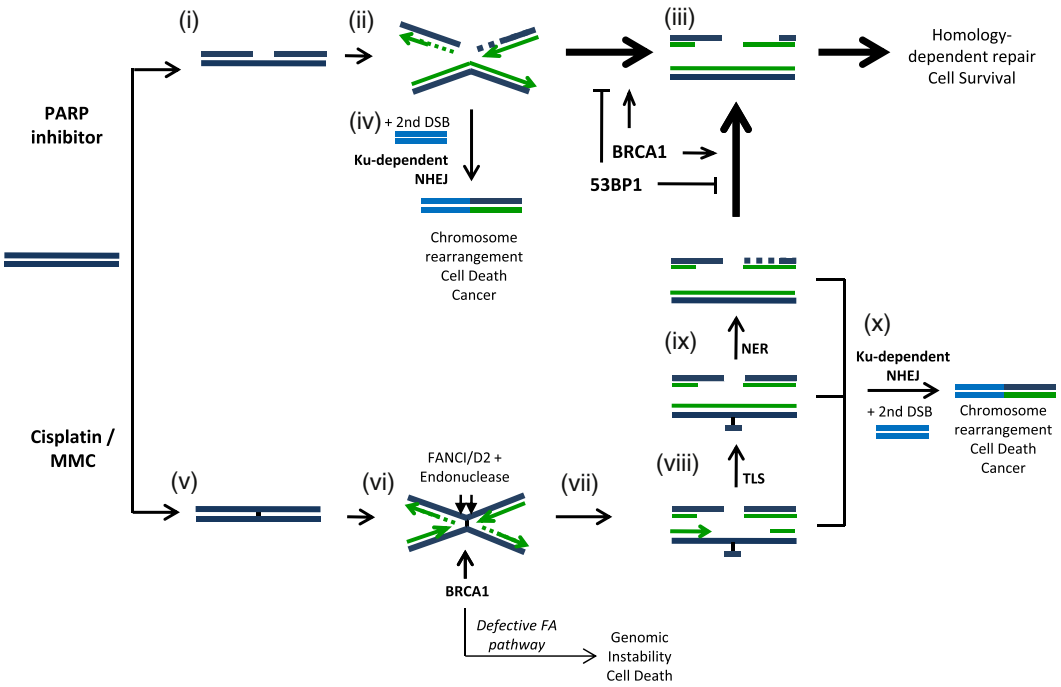

Figure 6. Model for Repair of DNA Double-Strand Breaks Induced by PARP Inhibitor or DNA Crosslinking Agents

In (i), treatment with PARP inhibitor stabilizes spontaneous DNA single-strand breaks, which are converted to double-strand breaks (DSBs) during DNA replication (Bryant et al., 2005; Farmer et al., 2005). In (ii), DNA DSBs can be repaired either by NHEJ or HR. In (iii), the 5′–3′ exonuclease resection commits repair to the error-free HR pathway. 53BP1 antagonizes double-strand break resection. In (iv), Ku70/80 can potentially join the DSB to a second DNA end present in the cells to cause chromosome rearrangements. In (v), treatment with cisplatin or MMC generates interstrand DNA crosslinks. In (vi), interstrand crosslinks cause replication fork stalling and collapse. Accumulation of FANCI/D2, dependent on BRCA1, recruits endonucleases that cut DNA on either side of the interstrand crosslink to generate a double-strand break (vii). Translesion synthesis (TLS) (viii) and nucleotide excision repair (NER) (ix) regenerate duplex DNA on one sister chromatid, enabling homology-dependent repair of the DNA DSB. In (x), aberrant joining mediated by Ku70/80 competes with normal repair and can potentially generate chromosome rearrangements leading to cancer or cell death.

Differing Requirements for BRCA1 and FANCD2 in Upstream ICL Repair

Our finding that *Brca1*$^{-/-}$*53BP1*$^{-/-}$ cells are HR competent but still hypersensitive to ICLs suggests that in addition to its established role in HR, BRCA1 has an upstream role in processing ICLs prior to DSB repair by HR (Figure 6, vi). BRCA1 has previously been reported to regulate the accumulation of FANCD2 into repair foci (Garcia-Higuera et al., 2001; Vandenberg et al., 2003). We found that FANCD2 foci are still impaired in Brca1$^{\Delta 11/\Delta 11}$53BP1$^{-/-}$ cells (Figure 4B), which may explain why loss of 53BP1 does not reduce the sensitivity of *Brca1*-deficient cells to DNA crosslinking agents. The requirement of BRCA1 for optimal retention of FANCD2 at the sites of ICL repair may be dependent on the reported ability of BRCA1 to promote chromatin unfolding (Ye et al., 2001), which may facilitate foci formation by monoubiquitylated FANCD2. Alternatively, BRCA1 may regulate signaling pathways downstream of DNA damage (such as ATR activation) (Yarden et al., 2002) or transcriptional events required for ICL repair (Aiyar et al., 2005; Zhu et al., 2011).

Depletion of Ku70/80 was able to reverse the defect in FANCD2 accumulation in *Brca1*-deficient cells (Figure 4B), suggesting that Ku70/80 and BRCA1 have antagonistic effects in regulating FANCD2 accumulation. Although the exact mechanism by which loss of Ku increases FANCD2 accumulation is unclear, one possibility is that Ku binding to DNA ends produced either by endonuclease excision of DNA crosslinks or by replication fork regression displaces FA gene products that are required for faithful repair at the crosslink site. Alternatively, Ku binding to DNA ends may prevent the action of a putative nuclease activity recently reported to be associated with FANCD2 (Pace et al., 2010).

Whereas *FANCD2*-deficient cells treated with DNA crosslinking agents accumulate additional genomic instability in the absence of Ku, *Brca1*-deficient cells show improved genomic stability and survival when Ku is depleted (Figures 2C–2E, 5C, and 5D). These data suggest that the role of BRCA1 in upstream ICL processing is not essential; BRCA1 rather has an accessory role in mediating optimal FANCD2 accumulation, as in the absence of BRCA1, FANCD2 foci after DNA crosslinking are reduced but not absent (Figure 4B). In contrast, FANCD2 is an essential player in ICL repair, and a deficiency in FANCD2 can therefore not be compensated by deletion of *53BP1* or *Ku.*

Two recent reports indicated that deletion of Ku promotes survival and restores genome integrity in cells deficient in the FA pathway (Adamo et al., 2010; Pace et al., 2010). Nevertheless, discordant results were obtained when testing the effects of various NHEJ mutants. For example, in chicken cells, it was

found that loss of DNA ligase IV (*Lig4*) in *FANCC* mutant cells caused additive repair defects, whereas loss of Ku suppressed the repair defects (Pace et al., 2010). The difference between our data and previously reported results may reflect the fact that DT40 cells used in earlier studies utilize HR for repair at a much higher frequency than other cell types, suggesting that different mechanisms could regulate DSB repair pathway choice in different model systems (Buerstedde and Takeda, 1991). Moreover, the function of FA proteins in mice and humans may be distinct, as several mouse models do not typically exhibit as severe congenital and hematopoietic abnormalities and cancer predisposition as in human patients. Nevertheless, based on our data on Ku deficiency and a corresponding study with *DNA-PKcs*$^{-/-}$ mice crossed with *FANCD2*$^{-/-}$ (Houghtaling et al., 2005) (Table S1), we do not believe it will be possible to relieve FA phenotypes by targeting NHEJ.

Secondary Mutations in *53BP1* and *Ku* as Potential Contributors to Chemoresistance

PARP inhibitors have shown considerable promise as targeted therapies for tumors with deficiencies in BRCA1 or BRCA2, and recent profiling of ovarian tumors has indicated that up to 50% of such cancer cases could be amenable to treatment with PARP inhibitors based on the presence of mutations that affect HR (Cancer Genome Atlas Research Network, 2011). Chemo resistance may arise in cancer cases treated with PARP inhibitor because of the presence of secondary mutations that reduce the sensitivity of HR-deficient tumor cells to PARP inhibition. We propose that mutations in *53BP1* and *Ku70/80* are candidates for altered drug sensitivity in HR-deficient tumors, and that characterization of the status of these genes is likely to have prognostic value in planning treatment with PARP inhibitors or platinum-based chemotherapy.

EXPERIMENTAL PROCEDURES

Mice

Mice carrying the *Brca1*$^{\Delta 11}$ allele were obtained from the NIH mouse repository. *Brca1*- and *Ku80*-null mice were obtained as described (Ludwig et al., 1997; Nussenzweig et al., 1996).

shRNA and Growth Assays

shRNA constructs were obtained from Open Biosystems. Twenty-four hours after lentiviral infection, stable integrants were selected with puromycin. Western blotting was performed using anti-Ku70 mouse monoclonal antibody (mab-Ku70, 3114-500, Abcam used at 1:500). For overexpression, rat Ku70 was subcloned (Yang et al., 1996) into the pMX retroviral vector for infection into passage-immortalized MEFs. For short-term growth assays, cells were grown continuously with PARP inhibitor or for 24 hr in the presence of cisplatin. Proliferation was assayed after 5 days with CellTiterGlo (Promega) according to the manufacturer's instructions. For colony formation, cells were grown for 14 days, then fixed with methanol and stained with crystal violet. Metaphase preparation and telomere FISH was as described (Callén et al., 2007). PARP inhibitor (KU58948) was obtained from Astra Zeneca.

Native BrdU Detection and RPA ChIP

Exponentially growing cells were pulsed with 1 μM BrdU (Sigma) for 36 hr, irradiated (30 Gy, 2 hr recovery at 37°C); then fixed with methanol at −20°C for 20 min. Cells were blocked in 3% BSA in PBS for 30 min, then stained with anti-BrdU monoclonal antibody for 1hr. Before analysis, propidium iodide was added to a final concentration of 20 μg/ml. RPA ChIP was performed as previously described (Yamane et al., 2011).

ACCESSION NUMBERS

GEO: ChIP-seq data for RPA, GSE35698.

SUPPLEMENTAL INFORMATION

Supplemental Information includes one table and five figures and can be found with this article online at doi:10.1016/j.molcel.2012.02.015.

ACKNOWLEDGMENTS

We thank Laura Niedernhofer, Jeremy Daniel, and Elise Kohn for helpful discussions and suggestions; Mark O'Connor for Parpi; and Michael Eckhaus and Mark Bryant for assistance with histology. The work was supported by the Intramural Research Program of the NIH, the National Cancer Institute, and the Center for Cancer Research, and by a Department of Defense grant to A.N. (BC102335) and a K99/R00 grant (1K99CA160574-01) to S.B. Research was conducted in compliance with the Animal Welfare Act Regulations and other federal statutes relating to animals and experiments involving animals and adheres to the principles set forth in the Guide for Care and Use of Laboratory Animals, National Research Council, 1996.

Received: September 9, 2011
Revised: January 13, 2012
Accepted: February 10, 2012
Published online: March 22, 2012

REFERENCES

Adamo, A., Collis, S.J., Adelman, C.A., Silva, N., Horejsi, Z., Ward, J.D., Martinez-Perez, E., Boulton, S.J., and La Volpe, A. (2010). Preventing nonhomologous end joining suppresses DNA repair defects of Fanconi anemia. Mol. Cell *39*, 25–35.

Aiyar, S., Sun, J.L., and Li, R. (2005). BRCA1: a locus-specific "liaison" in gene expression and genetic integrity. J. Cell. Biochem. *94*, 1103–1111.

Bhattacharyya, A., Ear, U.S., Koller, B.H., Weichselbaum, R.R., and Bishop, D.K. (2000). The breast cancer susceptibility gene BRCA1 is required for subnuclear assembly of Rad51 and survival following treatment with the DNA cross-linking agent cisplatin. J. Biol. Chem. *275*, 23899–23903.

Bothmer, A., Robbiani, D.F., Feldhahn, N., Gazumyan, A., Nussenzweig, A., and Nussenzweig, M.C. (2010). 53BP1 regulates DNA resection and the choice between classical and alternative end joining during class switch recombination. J. Exp. Med. *207*, 855–865.

Bothmer, A., Robbiani, D.F., Di Virgilio, M., Bunting, S.F., Klein, I.A., Feldhahn, N., Barlow, J., Chen, H.T., Bosque, D., Callen, E., et al. (2011). Regulation of DNA end joining, resection, and immunoglobulin class switch recombination by 53BP1. Mol. Cell *42*, 319–329.

Botuyan, M.V., Lee, J., Ward, I.M., Kim, J.E., Thompson, J.R., Chen, J., and Mer, G. (2006). Structural basis for the methylation state-specific recognition of histone H4-K20 by 53BP1 and Crb2 in DNA repair. Cell *127*, 1361–1373.

Bouwman, P., Aly, A., Escandell, J.M., Pieterse, M., Bartkova, J., van der Gulden, H., Hiddingh, S., Thanasoula, M., Kulkarni, A., Yang, Q., et al. (2010). 53BP1 loss rescues BRCA1 deficiency and is associated with triple-negative and BRCA-mutated breast cancers. Nat. Struct. Mol. Biol. *17*, 688–695.

Bryant, H.E., Schultz, N., Thomas, H.D., Parker, K.M., Flower, D., Lopez, E., Kyle, S., Meuth, M., Curtin, N.J., and Helleday, T. (2005). Specific killing of BRCA2-deficient tumours with inhibitors of poly(ADP-ribose) polymerase. Nature *434*, 913–917.

Buerstedde, J.M., and Takeda, S. (1991). Increased ratio of targeted to random integration after transfection of chicken B cell lines. Cell *67*, 179–188.

Bunting, S.F., Callén, E., Wong, N., Chen, H.T., Polato, F., Gunn, A., Bothmer, A., Feldhahn, N., Fernandez-Capetillo, O., Cao, L., et al. (2010). 53BP1 inhibits homologous recombination in Brca1-deficient cells by blocking resection of DNA breaks. Cell *141*, 243–254.

Callén, E., Jankovic, M., Difilippantonio, S., Daniel, J.A., Chen, H.T., Celeste, A., Pellegrini, M., McBride, K., Wangsa, D., Bredemeyer, A.L., et al. (2007). ATM prevents the persistence and propagation of chromosome breaks in lymphocytes. Cell *130*, 63–75.

Cancer Genome Atlas Research Network. (2011). Integrated genomic analyses of ovarian carcinoma. Nature *474*, 609–615.

Cao, L., Xu, X., Bunting, S.F., Liu, J., Wang, R.H., Cao, L.L., Wu, J.J., Peng, T.N., Chen, J., Nussenzweig, A., et al. (2009). A selective requirement for 53BP1 in the biological response to genomic instability induced by Brca1 deficiency. Mol. Cell *35*, 534–541.

Cobleigh, M.A. (2011). Other options in the treatment of advanced breast cancer. Semin. Oncol. *38* (*Suppl 2*), S11–S16.

Critchlow, S.E., and Jackson, S.P. (1998). DNA end-joining: from yeast to man. Trends Biochem. Sci. *23*, 394–398.

Difilippantonio, S., Gapud, E., Wong, N., Huang, C.Y., Mahowald, G., Chen, H.T., Kruhlak, M.J., Callen, E., Livak, F., Nussenzweig, M.C., et al. (2008). 53BP1 facilitates long-range DNA end-joining during V(D)J recombination. Nature *456*, 529–533.

Dimitrova, N., Chen, Y.C., Spector, D.L., and de Lange, T. (2008). 53BP1 promotes non-homologous end joining of telomeres by increasing chromatin mobility. Nature *456*, 524–528.

Farmer, H., McCabe, N., Lord, C.J., Tutt, A.N., Johnson, D.A., Richardson, T.B., Santarosa, M., Dillon, K.J., Hickson, I., Knights, C., et al. (2005). Targeting the DNA repair defect in BRCA mutant cells as a therapeutic strategy. Nature *434*, 917–921.

Garcia-Higuera, I., Taniguchi, T., Ganesan, S., Meyn, M.S., Timmers, C., Hejna, J., Grompe, M., and D'Andrea, A.D. (2001). Interaction of the Fanconi anemia proteins and BRCA1 in a common pathway. Mol. Cell *7*, 249–262.

Getts, R.C., and Stamato, T.D. (1994). Absence of a Ku-like DNA end binding activity in the xrs double-strand DNA repair-deficient mutant. J. Biol. Chem. *269*, 15981–15984.

Gravel, S., Chapman, J.R., Magill, C., and Jackson, S.P. (2008). DNA helicases Sgs1 and BLM promote DNA double-strand break resection. Genes Dev. *22*, 2767–2772.

Houghtaling, S., Timmers, C., Noll, M., Finegold, M.J., Jones, S.N., Meyn, M.S., and Grompe, M. (2003). Epithelial cancer in Fanconi anemia complementation group D2 (Fancd2) knockout mice. Genes Dev. *17*, 2021–2035.

Houghtaling, S., Newell, A., Akkari, Y., Taniguchi, T., Olson, S., and Grompe, M. (2005). Fancd2 functions in a double strand break repair pathway that is distinct from non-homologous end joining. Hum. Mol. Genet. *14*, 3027–3033.

Huang, M., and D'Andrea, A.D. (2010). A new nuclease member of the FAN club. Nat. Struct. Mol. Biol. *17*, 926–928.

Huertas, P. (2010). DNA resection in eukaryotes: deciding how to fix the break. Nat. Struct. Mol. Biol. *17*, 11–16.

Huyen, Y., Zgheib, O., Ditullio, R.A., Jr., Gorgoulis, V.G., Zacharatos, P., Petty, T.J., Sheston, E.A., Mellert, H.S., Stavridi, E.S., and Halazonetis, T.D. (2004). Methylated lysine 79 of histone H3 targets 53BP1 to DNA double-strand breaks. Nature *432*, 406–411.

Jensen, R., and Glazer, P.M. (2004). Cell-interdependent cisplatin killing by Ku/DNA-dependent protein kinase signaling transduced through gap junctions. Proc. Natl. Acad. Sci. USA *101*, 6134–6139.

Kass, E.M., and Jasin, M. (2010). Collaboration and competition between DNA double-strand break repair pathways. FEBS Lett. *584*, 3703–3708.

Kee, Y., and D'Andrea, A.D. (2010). Expanded roles of the Fanconi anemia pathway in preserving genomic stability. Genes Dev. *24*, 1680–1694.

Knipscheer, P., Räschle, M., Smogorzewska, A., Enoiu, M., Ho, T.V., Schärer, O.D., Elledge, S.J., and Walter, J.C. (2009). The Fanconi anemia pathway promotes replication-dependent DNA interstrand cross-link repair. Science *326*, 1698–1701.

Long, D.T., Räschle, M., Joukov, V., and Walter, J.C. (2011). Mechanism of RAD51-dependent DNA interstrand cross-link repair. Science *333*, 84–87.

Ludwig, T., Chapman, D.L., Papaioannou, V.E., and Efstratiadis, A. (1997). Targeted mutations of breast cancer susceptibility gene homologs in mice: lethal phenotypes of Brca1, Brca2, Brca1/Brca2, Brca1/p53, and Brca2/p53 nullizygous embryos. Genes Dev. *11*, 1226–1241.

Manis, J.P., Morales, J.C., Xia, Z., Kutok, J.L., Alt, F.W., and Carpenter, P.B. (2004). 53BP1 links DNA damage-response pathways to immunoglobulin heavy chain class-switch recombination. Nat. Immunol. *5*, 481–487.

Nussenzweig, A., and Nussenzweig, M.C. (2010). Origin of chromosomal translocations in lymphoid cancer. Cell *141*, 27–38.

Nussenzweig, A., Chen, C., da Costa Soares, V., Sanchez, M., Sokol, K., Nussenzweig, M.C., and Li, G.C. (1996). Requirement for Ku80 in growth and immunoglobulin V(D)J recombination. Nature *382*, 551–555.

Pace, P., Mosedale, G., Hodskinson, M.R., Rosado, I.V., Sivasubramaniam, M., and Patel, K.J. (2010). Ku70 corrupts DNA repair in the absence of the Fanconi anemia pathway. Science *329*, 219–223.

Patel, A.G., Sarkaria, J.N., and Kaufmann, S.H. (2011). Nonhomologous end joining drives poly(ADP-ribose) polymerase (PARP) inhibitor lethality in homologous recombination-deficient cells. Proc. Natl. Acad. Sci. USA *108*, 3406–3411.

Pierce, A.J., Hu, P., Han, M., Ellis, N., and Jasin, M. (2001). Ku DNA end-binding protein modulates homologous repair of double-strand breaks in mammalian cells. Genes Dev. *15*, 3237–3242.

Rathmell, W.K., and Chu, G. (1994). A DNA end-binding factor involved in double-strand break repair and V(D)J recombination. Mol. Cell. Biol. *14*, 4741–4748.

Sartori, A.A., Lukas, C., Coates, J., Mistrik, M., Fu, S., Bartek, J., Baer, R., Lukas, J., and Jackson, S.P. (2007). Human CtIP promotes DNA end resection. Nature *450*, 509–514.

Stracker, T.H., and Petrini, J.H. (2011). The MRE11 complex: starting from the ends. Nat. Rev. Mol. Cell Biol. *12*, 90–103.

Taccioli, G.E., Gottlieb, T.M., Blunt, T., Priestley, A., Demengeot, J., Mizuta, R., Lehmann, A.R., Alt, F.W., Jackson, S.P., and Jeggo, P.A. (1994). Ku80: product of the XRCC5 gene and its role in DNA repair and V(D)J recombination. Science *265*, 1442–1445.

Vandenberg, C.J., Gergely, F., Ong, C.Y., Pace, P., Mallery, D.L., Hiom, K., and Patel, K.J. (2003). BRCA1-independent ubiquitination of FANCD2. Mol. Cell *12*, 247–254.

Wang, W. (2007). Emergence of a DNA-damage response network consisting of Fanconi anaemia and BRCA proteins. Nat. Rev. Genet. *8*, 735–748.

Wang, B., Matsuoka, S., Ballif, B.A., Zhang, D., Smogorzewska, A., Gygi, S.P., and Elledge, S.J. (2007). Abraxas and RAP80 form a BRCA1 protein complex required for the DNA damage response. Science *316*, 1194–1198.

Ward, I.M., Minn, K., van Deursen, J., and Chen, J. (2003). p53 Binding protein 53BP1 is required for DNA damage responses and tumor suppression in mice. Mol. Cell. Biol. *23*, 2556–2563.

Xu, X., Wagner, K.U., Larson, D., Weaver, Z., Li, C., Ried, T., Hennighausen, L., Wynshaw-Boris, A., and Deng, C.X. (1999a). Conditional mutation of Brca1 in mammary epithelial cells results in blunted ductal morphogenesis and tumour formation. Nat. Genet. *22*, 37–43.

Xu, X., Weaver, Z., Linke, S.P., Li, C., Gotay, J., Wang, X.W., Harris, C.C., Ried, T., and Deng, C.X. (1999b). Centrosome amplification and a defective G2-M cell cycle checkpoint induce genetic instability in BRCA1 exon 11 isoform-deficient cells. Mol. Cell *3*, 389–395.

Xu, X., Qiao, W., Linke, S.P., Cao, L., Li, W.M., Furth, P.A., Harris, C.C., and Deng, C.X. (2001). Genetic interactions between tumor suppressors Brca1 and p53 in apoptosis, cell cycle and tumorigenesis. Nat. Genet. *28*, 266–271.

Yamane, A., Resch, W., Kuo, N., Kuchen, S., Li, Z., Sun, H.W., Robbiani, D.F., McBride, K., Nussenzweig, M.C., and Casellas, R. (2011). Deep-sequencing

identification of the genomic targets of the cytidine deaminase AID and its cofactor RPA in B lymphocytes. Nat. Immunol. *12*, 62–69.

Yang, S.H., Nussenzweig, A., Yang, W.H., Kim, D., and Li, G.C. (1996). Cloning and characterization of rat Ku70: involvement of Ku autoantigen in the heat-shock response. Radiat. Res. *146*, 603–611.

Yarden, R.I., Pardo-Reoyo, S., Sgagias, M., Cowan, K.H., and Brody, L.C. (2002). BRCA1 regulates the G2/M checkpoint by activating Chk1 kinase upon DNA damage. Nat. Genet. *30*, 285–289.

Ye, Q., Hu, Y.F., Zhong, H., Nye, A.C., Belmont, A.S., and Li, R. (2001). BRCA1-induced large-scale chromatin unfolding and allele-specific effects of cancer-predisposing mutations. J. Cell Biol. *155*, 911–921.

Yun, M.H., and Hiom, K. (2009). CtIP-BRCA1 modulates the choice of DNA double-strand-break repair pathway throughout the cell cycle. Nature *459*, 460–463.

Zhang, Q.S., Marquez-Loza, L., Eaton, L., Duncan, A.W., Goldman, D.C., Anur, P., Watanabe-Smith, K., Rathbun, R.K., Fleming, W.H., Bagby, G.C., and Grompe, M. (2010). Fancd2-/- mice have hematopoietic defects that can be partially corrected by resveratrol. Blood *116*, 5140–5148.

Zhu, Q., Pao, G.M., Huynh, A.M., Suh, H., Tonnu, N., Nederlof, P.M., Gage, F.H., and Verma, I.M. (2011). BRCA1 tumour suppression occurs via heterochromatin-mediated silencing. Nature *477*, 179–184.

Molecular Cell
Article

Regulation of DNA End Joining, Resection, and Immunoglobulin Class Switch Recombination by 53BP1

Anne Bothmer,[1,4] Davide F. Robbiani,[1,4] Michela Di Virgilio,[1] Samuel F. Bunting,[3] Isaac A. Klein,[1] Niklas Feldhahn,[1] Jacqueline Barlow,[3] Hua-Tang Chen,[3] David Bosque,[1] Elsa Callen,[3] André Nussenzweig,[3,5,*] and Michel C. Nussenzweig[1,2,5,*]
[1]Laboratory of Molecular Immunology
[2]Howard Hughes Medical Institute
The Rockefeller University, New York, NY 10065, USA
[3]Experimental Immunology Branch, National Cancer Institute, National Institutes of Health, Bethesda, MD 20892, USA
[4]These authors contributed equally to this work
[5]These authors contributed equally to this work
*Correspondence: nussenza@exchange.nih.gov (A.N.), nussen@mail.rockefeller.edu (M.C.N.)
DOI 10.1016/j.molcel.2011.03.019

SUMMARY

53BP1 is a DNA damage protein that forms phosphorylated H2AX (γ-H2AX) dependent foci in a 1 Mb region surrounding DNA double-strand breaks (DSBs). In addition, 53BP1 promotes genomic stability by regulating the metabolism of DNA ends. We have compared the joining rates of paired DSBs separated by 1.2 kb to 27 Mb on chromosome 12 in the presence or absence of 53BP1. 53BP1 facilitates joining of intrachromosomal DSBs but only at distances corresponding to γ-H2AX spreading. In contrast, DNA end protection by 53BP1 is distance independent. Furthermore, analysis of 53BP1 mutants shows that chromatin association, oligomerization, and N-terminal ATM phosphorylation are all required for DNA end protection and joining as measured by immunoglobulin class switch recombination. These data elucidate the molecular events that are required for 53BP1 to maintain genomic stability and point to a model wherein 53BP1 and H2AX cooperate to repress resection of DSBs.

INTRODUCTION

53BP1 is a DNA damage response protein that rapidly forms nuclear foci in response to DNA damage (Anderson et al., 2001; Rappold et al., 2001; Schultz et al., 2000). This process is dependent on PIKK- (ATM/ATR/DNA-PKcs) induced phosphorylation of histone H2AX (γ-H2AX) (Celeste et al., 2003; Fernandez-Capetillo et al., 2002; Ward et al., 2003; Yuan and Chen, 2010). γ-H2AX in turn recruits the E3 ubiquitin ligases RNF8 and RNF168 (Doil et al., 2009; Huen et al., 2007; Kolas et al., 2007; Mailand et al., 2007; Stewart et al., 2009), which promote histone ubiquitylation at sites of double-strand breaks (DSBs). The way in which ubiquitylation facilitates the accumulation of 53BP1 at sites of DSBs has not yet been defined, but one possible scenario is that ubiquitylation exposes constitutive chromatin marks, such as H4K20^{me2}, to which 53BP1 then binds via its tandem tudor domain (Botuyan et al., 2006; Mailand et al., 2007).

In addition to its chromatin-binding tudor domain, 53BP1 contains an oligomerization domain, tandem BRCA1 C-terminal (BRCT) domains, and numerous sites that can be modified post-translationally (Adams and Carpenter, 2006). Homo-oligomerization and interaction between the tudor domains and H4K20^{me2} are required for 53BP1 focus formation in response to DNA damage (Botuyan et al., 2006; Iwabuchi et al., 2003; Ward et al., 2003, 2006; Zgheib et al., 2009). In contrast, the C-terminal tandem BRCT domains are not essential for focus formation but mediate the interaction between 53BP1 and EXPAND1, a protein shown to promote chromatin changes after DNA damage and to facilitate repair (Huen et al., 2010; Ward et al., 2006). Finally, the N-terminal portion of 53BP1 lacks defined structural domains but contains multiple S/T-Q motifs, which are phosphorylation targets of ATM. Although mutating these residues to alanine alters the kinetics of resolution of DNA damage foci, it does not affect the formation of 53BP1 foci in response to DNA damage (DiTullio et al., 2002; Morales et al., 2003; Ward et al., 2006).

In addition to DNA damage-dependent focus formation, 53BP1 is required to protect DSBs from end resection (Bothmer et al., 2010; Bunting et al., 2010). The absence of 53BP1 facilitates resection, thereby relieving a block to homologous recombination in Brca1 mutant cells, promoting degradation of DNA ends during V(D)J recombination and promoting microhomology-mediated alternative NHEJ (A-NHEJ) during immunoglobulin class switch recombination (CSR) (Bothmer et al., 2010; Bunting et al., 2010; Difilippantonio et al., 2008). CSR is a B cell-specific antibody diversification reaction leading to the production of antibodies of different isotypes with altered effector functions (Manis et al., 2004; Ward et al., 2004). Mechanistically CSR is a deletional recombination reaction between paired DSBs in highly repetitive *Ig* switch regions (S regions) separated by 60–200 kb (Stavnezer et al., 2008). Each S region contains a characteristic repetitive sequence, which can also

serve as a substrate for proximal microhomology-mediated intraswitch repair by A-NHEJ at the expense of CSR (Boboila et al., 2010a, 2010b; Bothmer et al., 2010; Reina-San-Martin et al., 2007). Efficient rearrangements require synapsis and repair by classical-NHEJ (C-NHEJ). In addition to CSR, 53BP1 is also required for the joining of distal DSBs during V-J recombination at the TCRα locus (Difilippantonio et al., 2008), and for the fusion of deprotected telomeres (Dimitrova et al., 2008).

Several non-mutually exclusive models have been put forward to explain how 53BP1 helps maintain genome stability and contributes to CSR. One model proposes that 53BP1 facilitates distal DSB joining by synapsing paired DSBs, either by altering local chromatin structure or by increasing chromatin mobility (Difilippantonio et al., 2008; Dimitrova et al., 2008). 53BP1 may also favor CSR by protecting DSBs in Ig switch regions from resection, thereby limiting A-NHEJ mediated intraswitch recombination between homologous sequences while promoting productive interswitch rearrangements by C-NHEJ (Bothmer et al., 2010).

Here, we show that the effects of 53BP1 on joining depend on the distance between the broken ends while DNA end protection by 53BP1 is a distance independent function. We furthermore define the domains of 53BP1 that are required for CSR and DNA end protection.

RESULTS

Role of Distance in Joining of DSBs

During CSR, activation-induced cytidine deaminase (AID) produces tandem DSBs in Ig heavy chain (IgH) switch regions separated by 60–200 kb. 53BP1 is required for the efficient joining between IgH switch breaks and similarly facilitates the joining of I-SceI-induced DSBs separated by 96 kb (Bothmer et al., 2010). To determine how distance affects the joining efficiency of paired DSBs on the chromosome bearing the IgH locus, we produced additional knockin mice bearing I-SceI sites separated by 1.2 kb or 27 Mb on chromosome 12 ($IgH^{I\text{-}1k}$ and $IgH^{I\text{-}27M}$, respectively; Figures S1A and S1D available online). $IgH^{I\text{-}1k}$ and $IgH^{I\text{-}27M}$ showed normal B cell development and CSR to IgG1 upon stimulation with LPS and IL4 (Figures S1B and S1E).

To compare the joining efficiency of DSBs at different distances on the same chromosome, we infected $IgH^{I\text{-}1k/+}AID^{-/-}$ and $IgH^{I\text{-}27M/+}AID^{-/-}$ B cells with an I-SceI-expressing virus or an inactive I-SceI* control and measured recombination frequencies by sample dilution PCR (Figure S1C). Strikingly, the efficiency of joining DSBs separated by 27 Mb was >30-fold lower than that of DSBs separated by 1.2 kb (0.0048×10^{-2} versus 0.17×10^{-2}, $p < 0.0001$, gray bars in Figures 1E and 1B) or 96 kb (0.7×10^{-2}) (Bothmer et al., 2010). To determine how distal intrachromosomal repair compares with transchromosomal joining, we produced mice with paired I-SceI sites on chromosomes 12 and 15 (IgH^{I} and Myc^{I}, respectively) (Robbiani et al., 2008) and generated translocations by infecting cells with I-SceI viruses. The joining frequency of I-SceI-infected $IgH^{I/+}Myc^{I/+}AID^{-/-}$ B cells was 0.0027×10^{-2} per cell, which is comparable to the joining between I-SceI sites separated by 27 Mb in $IgH^{I\text{-}27M/+}AID^{-/-}$ (Figures 1E and 1H, gray bars). We conclude that the joining of proximal (1.2 or 96 kb) intrachromosomal DSBs is significantly more efficient than distal (27 Mb) intrachromosomal joining, and that the latter is similar to transchromosomal joining.

Loss of 53BP1 decreases the joining efficiency of I-SceI-induced DSBs separated by 96 kb at the IgH locus, although the effect is less pronounced than for AID-mediated CSR (Bothmer et al., 2010). To determine the role of 53BP1 in distal versus proximal repair of paired DSBs, we compared joining between I-SceI sites in 53BP1 deficient $IgH^{I\text{-}1k}$ (proximal), $IgH^{I\text{-}27M}$ (distal), and $IgH^{I}Myc^{I}$ (interchromosomal) B cells ($IgH^{I\text{-}1k/+}AID^{-/-}53BP1^{-/-}$, $IgH^{I\text{-}27M/+}AID^{-/-}53BP1^{-/-}$, and $Myc^{I/+}IgH^{I/+}AID^{-/-}53BP1^{-/-}$ B cells, respectively). In contrast to the joining of DSBs separated by 96 kb (Bothmer et al., 2010), the absence of 53BP1 did not reduce the frequency of joining between I-SceI sites separated by 1.2 kb or 27 Mb on the same chromosome or sites on different chromosomes. (Figures 1B, 1E, and 1H and Figures S1F–S1H). We conclude that in contrast to facilitating the joining of DSBs separated by 96 kb, the loss of 53BP1 does not alter the joining frequency of more proximal or distal DSBs.

The loss of 53BP1 results in increased DNA end resection (Bothmer et al., 2010). To determine whether this effect is dependent on distance, we measured end resection in $IgH^{I\text{-}1k/+}AID^{-/-}53BP1^{-/-}$ and $IgH^{I\text{-}27M/+}AID^{-/-}53BP1^{-/-}$ B cells and the respective 53BP1-proficient controls. Joins with deletions of more than 35 nt (indicative of extensive end processing) increased from 37.2% in $IgH^{I\text{-}1k/+}AID^{-/-}$ to 52.4% in $IgH^{I\text{-}1k/+}AID^{-/-}53BP1^{-/-}$ and from 55.5% in $IgH^{I\text{-}27M/+}AID^{-/-}$ to 75.5% in $IgH^{I\text{-}27M/+}AID^{-/-}53BP1^{-/-}$ (Figures 1C and 1F). We conclude that 53BP1's ability to prevent end resection is independent of the distance between paired DSBs.

In summary, 53BP1 has a distance-independent function in the prevention of DNA end resection and a distance-dependent function in facilitating the joining of DSBs.

BRCT Domains

To investigate the function of the BRCT domains of 53BP1 in CSR, we deleted the region corresponding to amino acids 1708–1969 from the mouse germline ($53BP1^{\Delta BRCT}$; Figure 2A and Figure S2A). Lymphocyte development and CSR were normal in $53BP1^{\Delta BRCT}$ mice, despite lower than wild-type levels of the mutant protein (Figures 2B and 2C and Figure S2B).

To determine whether the BRCT domains are required for DSB end protection, we produced $53BP1^{\Delta BRCT/-}IgH^{I\text{-}96k/+}$ mice and assayed the resection of paired I-SceI breaks. We found a minor increase in DNA end resection compared to controls, which is probably due to the decreased expression level of the mutant protein (Figures 2B and 2D). We conclude that the BRCT domains of 53BP1 are dispensable for CSR and the protection of DNA ends from resection.

53BP1 Chromatin Association

53BP1 binds to $H4K20^{me2}$, a constitutive histone modification, and forms nuclear foci in response to DNA damage (Botuyan et al., 2006; Schultz et al., 2000). To determine whether 53BP1 is chromatin associated in B cells, we fractionated unstimulated B cells before or after treatment with ionizing radiation (IR). We found that a portion of the total cellular 53BP1 is chromatin associated in the steady-state even in the absence of DNA damage (Figure 3A). This is consistent with the finding that 53BP1

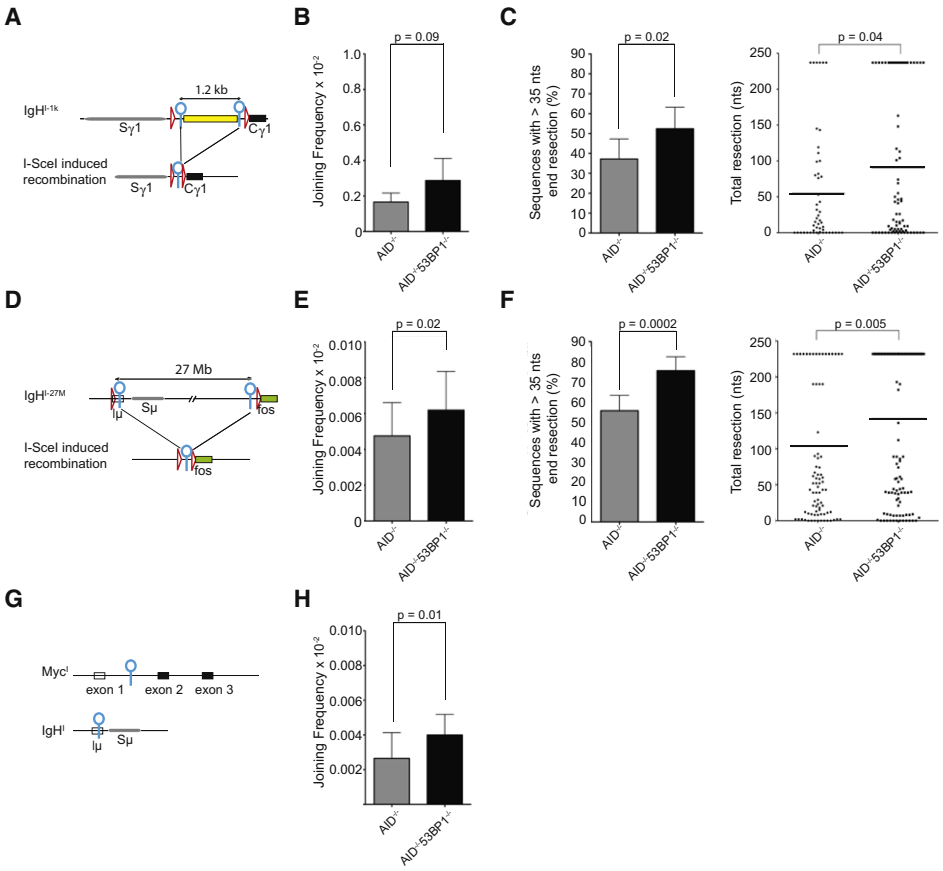

Figure 1. 53BP1 Effects on Joining of Proximal or Distal DSBs

(A) Schematic representation of IgH$^{I\text{-}1k}$ allele before (top) and after (bottom) I-SceI-induced recombination. I-SceI sites are indicated as blue circles and loxP sites as red triangles. Spacer sequence of 1.2 kb is indicated as yellow rectangle.

(B) Bar graph shows I-SceI-induced recombination frequency of IgH$^{I\text{-}1k/+}$AID$^{-/-}$ B cells in the presence or absence of 53BP1. p value was calculated with a paired two-tailed Student's t test. See also Figure S1F.

(C) Left: Bar graph showing the frequency of I-SceI-induced recombination products with more than 35 nt end processing for IgH$^{I\text{-}1k/+}$AID$^{-/-}$ and IgH$^{I\text{-}1k/+}$AID$^{-/-}$ 53BP1$^{-/-}$ B cells. Right: Dot plot showing resection in sequences from I-SceI-infected IgH$^{I\text{-}1k/+}$AID$^{-/-}$ and IgH$^{I\text{-}1k/+}$AID$^{-/-}$53BP1$^{-/-}$ B cells, with each dot representing one cloned sequence.

(D) Schematic representation of IgH$^{I\text{-}27M}$ allele before (top) and after (bottom) I-SceI-induced recombination.

(E) As in (B) for IgH$^{I\text{-}27M/+}$AID$^{-/-}$ and IgH$^{I\text{-}27M/+}$AID$^{-/-}$53BP1$^{-/-}$ B cells. See also Figure S1G.

(F) As in (C) for IgH$^{I\text{-}27M/+}$AID$^{-/-}$ and IgH$^{I\text{-}27M/+}$AID$^{-/-}$53BP1$^{-/-}$ B cells.

(G) Schematic representation of the Myc^{I} and IgH^{I} alleles.

(H) As in (B and E) for IgH$^{I/+}$Myc$^{I/+}$AID$^{-/-}$ B cells in the presence and absence of 53BP1. See also Figure S1H.

Horizontal lines in dot plots indicate the means. Error bars indicate standard deviations. p values were calculated using a two-tailed Student's t test, unless otherwise indicated. All graphs represent data from at least three independent experiments, unless specified. See also Figure S1.

constitutively associates with chromatin in a manner independent of RNF8 (Santos et al., 2010). Furthermore, chromatin association did not increase significantly after irradiation.

Residue D1521 in the tudor domain of 53BP1 is required for binding to H4K20^{me2} (Botuyan et al., 2006). To test the role of this interaction in CSR and DNA resection, we produced D1518R mutant mice (53BP1^{DR}) bearing a single amino acid substitution that is equivalent to D1521R in humans (Figure 3B and Figure S3A). Lymphocyte development was similar to the wild-type in 53BP1^{DR} mice (Figure S3B), and the mutant 53BP1^{DR} protein was normally phosphorylated at Ser^{25} upon IR (Figure S3C). In agreement with previous studies, 53BP1^{DR} failed to form IR-induced foci and showed only faint accumulation at sites of laser scissor damage in mouse embryonic fibroblasts (MEFs; Figure 3C and Figure S3D) (Botuyan et al., 2006; Huyen et al., 2004). In addition, 53BP1^{DR} was not chromatin associated in B cells (Figure 3D). We conclude that 53BP1 binds to chromatin constitutively through residue D1518 and that chromatin association is not required for 53BP1 phosphorylation.

To determine whether chromatin association is required for CSR, we stimulated 53BP1^{DR} B cells in vitro. Mutant B cells switched at about 10% of wild-type levels, phenocopying 53BP1$^{-/-}$ (Figure 3E). Loss of chromatin association also resulted in an increase in DNA end resection in 53BP1^{DR}IgH$^{I\text{-}96k/+}$ comparable to 53BP1$^{-/-}$IgH$^{I\text{-}96k/+}$ controls (Figure 3F). We conclude that 53BP1 is constitutively chromatin associated and

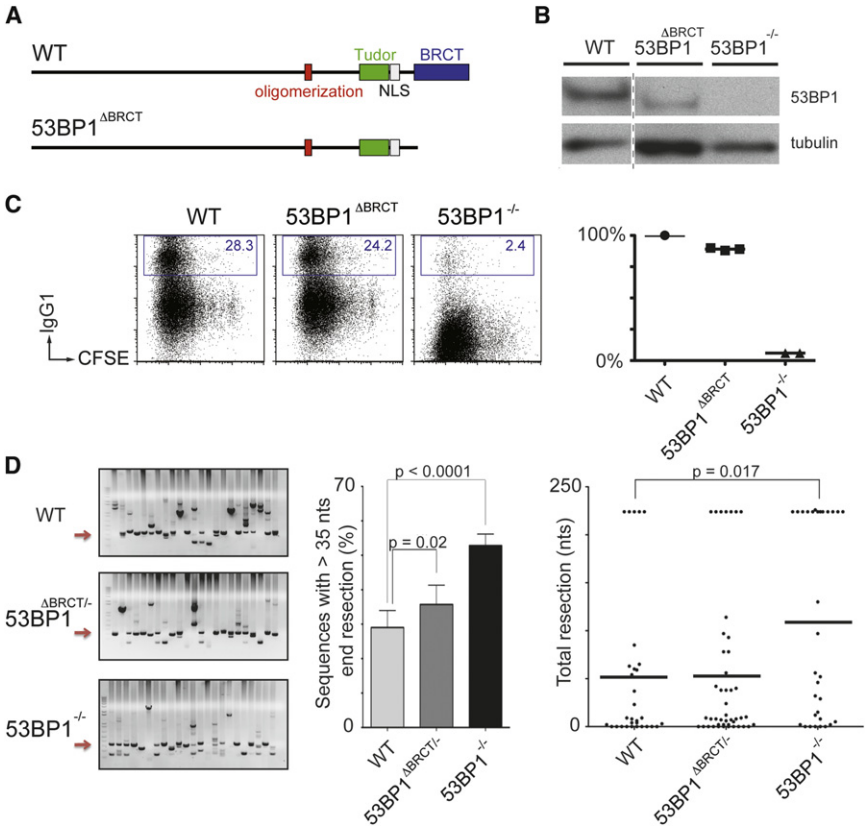

Figure 2. The BRCT Domains Are Dispensable for CSR and DNA End Protection

(A) Schematic representation of wild-type (WT) 53BP1 protein (top) and 53BP1 lacking the BRCT domains (bottom).

(B) Western blot showing 53BP1 expression levels in WT and 53BP1$^{\Delta BRCT}$ B cells.

(C) Left: Representative flow cytometry plots measuring CSR after stimulation of WT, 53BP1$^{\Delta BRCT}$ and 53BP1$^{-/-}$ B cells. Numbers indicate the percentage of IgG1 switched cells. CFSE dye tracks cell division. Right: Summary dot plot indicating CSR as a percentage of WT value within the same experiment. Each dot represents an independent experiment.

(D) Left: Representative ethidium bromide stained agarose gels showing PCR products obtained after I-SceI-induced recombination in IgH$^{I\text{-}96k/+}$, IgH$^{I\text{-}96k/+}$53BP1$^{\Delta BRCT/-}$, and IgH$^{I\text{-}96k}$53BP1$^{-/-}$ B cells. Middle: Bar graph quantitating the frequency of I-SceI-induced recombination products with more than 35 nt end processing. Error bars indicate standard deviation. Right: Dot plot showing resection with each dot representing one sequence. Two independent experiments.

See also Figure S2.

that this association is required for CSR and for the protection of DNA ends from resection.

H2AX Protects DNA Ends from Resection

H2AX is required for stable 53BP1 DNA damage focus formation, and its deficiency impairs CSR, but to a lesser extent than absence of 53BP1 (Celeste et al., 2002; Fernandez-Capetillo et al., 2002; Reina-San-Martin et al., 2003). Moreover, 53BP1 was reported to interact with H2AX (Ward et al., 2003). To determine whether the chromatin association of 53BP1 depends on this histone variant, we assayed H2AX-deficient B cells. Although H2AX is required for 53BP1 foci, we found that H2AX is dispensable for 53BP1 chromatin association (Figure 4A). To determine whether H2AX is required to prevent DNA resection, we assayed IgH$^{I\text{-}96k/+}$AID$^{-/-}$ H2AX$^{-/-}$ B cells. We found that resection was increased in the absence of H2AX to levels comparable to 53BP1$^{-/-}$ (51.7% compared to 35.8% in IgH$^{I\text{-}96k}$AID$^{-/-}$ control, Figure 4B). Interestingly, while allowing for resection, absence of H2AX does not reverse radial fusions that are observed in PARP inhibitor- (KU58948) treated Brca1 mutant cells (Figure 4C). Thus, although 53BP1 can be constitutively chromatin associated in the absence of H2AX, this alone is not sufficient to prevent the extensive resection.

The Oligomerization Domain of 53BP1 Is Required for CSR

The central region of 53BP1 is required for 53BP1 oligomerization (Ward et al., 2006; Zgheib et al., 2009) and contains residues that are phosphorylated by ATM (S1219) (Lee et al., 2009), ubiquitylated by Rad18 (K1268) (Watanabe et al., 2009), and methylated by PRMT1 (R1398, R1400, R1401) (Boisvert et al., 2005). To determine the role of this region in vivo, we produced mice that express a mutant form of 53BP1 lacking this region (Figure 5A and Figure S4A). 53BP1$^{\Delta 1210-1447}$ protein was expressed at normal levels, and lymphocyte development in 53BP1$^{\Delta 1210\text{-}1447}$ mice was similar to wild-type (Figures S4B and S4C).

However, 53BP1$^{\Delta 1210-1447}$ B cells are similar to null mutant cells in CSR (Figure 5B). To confirm this result and identify the responsible activity, we produced four region-specific mutant retroviruses and assayed them for their ability to rescue IgG1 switching in 53BP1$^{-/-}$ B cells (Figure 5C and 5D and Figure S4D; since full-length 53BP1 cannot be expressed by retroviruses, deletion of the BRCT domain, which is similar to wild-type [see Figure 2] can be used for retroviral expression). 53BP1$^{\Delta 1231-1270}$, which lacks the oligomerization domain, was the only mutant that failed to rescue CSR, despite partially retaining the ability to bind chromatin (Figure 5D and 5E) (Zgheib et al., 2009). We conclude that the oligomerization domain in 53BP1 is required for class switch recombination but that residues S1219, K1268, and R1398/R1400/R1401 are not.

Residues 1052 to 1710 of 53BP1 include the tudor and oligomerization domains, which are sufficient for chromatin binding and DNA damage focus formation (Figure 5F) (Ward et al., 2003; Zgheib et al., 2009). However, retrovirally expressed 53BP1$^{1052-1710}$ was unable to rescue CSR (Figure 5G and Figure S4E). We conclude that chromatin binding, oligomerization, and focus formation are insufficient to promote CSR, suggesting that the N terminus of 53BP1 may play an important role in this reaction.

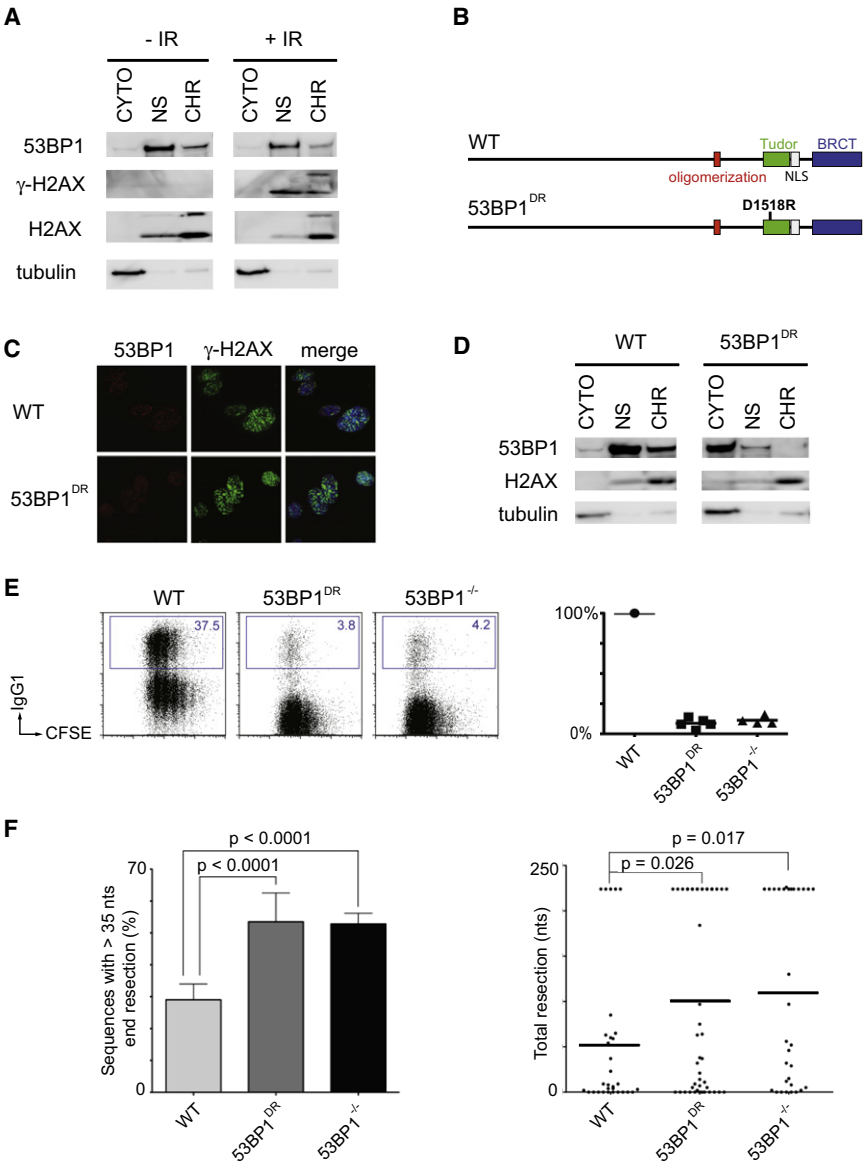

Figure 3. 53BP1 Tudor Domains Are Required for CSR and for the Protection of DNA Ends

(A) Western blots of fractionated WT B cells ± 10 Gy of IR. CYTO, cytoplasmic fraction; NS, nuclear soluble fraction; CHR, chromatin fraction.

(B) Schematic representation of WT 53BP1 (top) and 53BP1 with tudor domain mutation D1518R (bottom).

(C) 53BP1 and γ-H2AX IRIF in WT and 53BP1^{DR} MEFs after IR.

(D) Western blots of unstimulated, fractionated WT, and 53BP1^{DR} B cells.

(E) Left: Representative flow cytometry plots measuring CSR to IgG1 after stimulation of WT, 53BP1^{DR}, and 53BP1$^{-/-}$ B cells. Right: Summary dot plot indicating CSR as a percentage of WT. Each dot represents an independent experiment.

(F) As in Figure 1C for WT, 53BP1^{DR}, and 53BP1$^{-/-}$ B cells. Error bars indicate standard deviation. Two independent experiments.

See also Figure S3.

Phosphorylation Sites at the N Terminus of 53BP1

To examine the role of the N terminus of 53BP1 in CSR, we produced and tested additional mutants, including (1) smaller N-terminal deletions (53BP1$^{901–1710}$ and 53BP1$^{459–1710}$), (2) internal deletions corresponding to the amino acids encoded by exons 3–12 (53BP1$^{\Delta 61–901}$), 7–12 (53BP1$^{\Delta 216–901}$), and 12 alone (53BP1$^{\Delta 459–901}$), and (3) alanine substitution mutants of S/T-Q consensus sites for ATM phosphorylation (53BP1^{8A}, 53BP1^{7A}, 53BP1^{15A}, 53BP1^{28A}) (Morales et al., 2003; Ward et al., 2006). We found that all of the deletion mutants were unable to rescue CSR (Figures S5A and S5B). The alanine substitution mutants 53BP1^{8A}, 53BP1^{7A}, 53BP1^{15A}, and 53BP1^{28A} displayed a phenotype that correlated with the number of substitutions. 53BP1^{8A} showed 90% of WT CSR, whereas 53BP1^{28A} was similar to the null mutant (Figures 6A and 6B and Figure S5C). Despite its inability to rescue CSR, 53BP1^{28A} bound to chromatin and formed IR foci (Figures 6C and 6D). We conclude that multiple S/T-Q target sites for ATM phosphorylation at the N terminus of 53BP1 are required for CSR.

The Oligomerization Domain and N-Terminal Phosphorylation Sites in 53BP1 Protect DNA Ends from Processing

Loss of 53BP1 rescues homologous recombination in Brca1 mutant cells by facilitating the processing of DNA ends (Bunting et al., 2010). To determine which domains of 53BP1 are required for DNA end protection in Brca1 mutant cells, we infected Brca1$^{\Delta 11/\Delta 11}$53BP1$^{-/-}$ B cells with 53BP1 mutant retroviruses and measured the frequency of radial chromosome structures upon treatment with the PARP inhibitor (Bunting et al., 2010). Whereas 12 radial structures were found among 100 metaphases in Brca1$^{\Delta 11/\Delta 11}$53BP1$^{-/-}$ B cells infected with a negative control virus, 54 were present upon infection with 53BP1$^{1–1710}$ (average of two independent experiments, Figure 7A and Figure S6). Confirming our previous finding with 53BP1^{DR} B cells showing that chromatin binding is required for protection from DNA resection, a 53BP1^{D1521R} virus did not rescue radial formation (7/100 metaphases), nor did 53BP1$^{1052–1710}$ (10/100 metaphases), the oligomerization mutant 53BP1$^{\Delta 1231–1270}$ (12/100 metaphases), nor the alanine mutant 53BP1^{28A} (14/100 metaphases; Figure 7A). We conclude that the tudor and oligomerization domains and the S/T-Q sites at the N terminus of 53BP1 are required for end protection and contribute to 53BP1-mediated toxicity in Brca1 mutant cells.

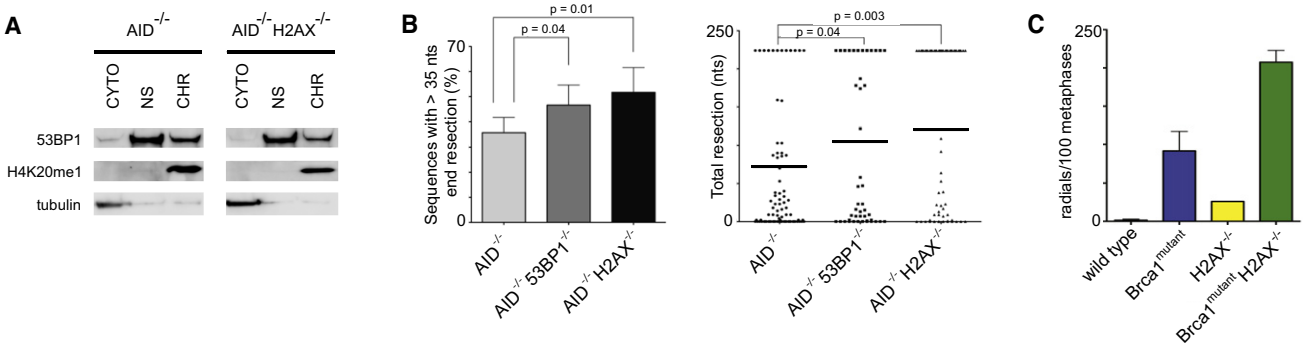

Figure 4. 53BP1 Chromatin Association in the Absence of H2AX Is Not Sufficient to Prevent End Resection

(A) Western blots of fractionated $AID^{-/-}$ and $AID^{-/-}H2AX^{-/-}$ B cells.

(B) Left: Bar graph showing the frequency of I-SceI-induced recombination products with more than 35 nt end processing for $IgH^{I\text{-}96k/+}AID^{-/-}$, $IgH^{I\text{-}96k/+}AID^{-/-}53BP1^{-/-}$, and $IgH^{I\text{-}96k/+}AID^{-/-}H2AX^{-/-}$ B cells. Right: Dot plot showing resection in sequences from I-SceI-infected $IgH^{I\text{-}96k/+}AID^{-/-}$, $IgH^{I\text{-}96k/+}AID^{-/-}53BP1^{-/-}$, and $IgH^{I\text{-}96k/+}AID^{-/-}H2AX^{-/-}$ B cells. Error bars indicate standard error of the mean. Two independent experiments.

(C) Histogram with number of radial structures in metaphases from PARP inhibitor-treated $Brca1^{lox/lox}CD19^{cre/+}$ ($Brca1^{mutant}$) B cells either proficient or deficient for H2AX. Error bars indicate standard error of the mean. Two independent experiments.

DISCUSSION

DNA breaks jeopardize genomic integrity, yet they occur as byproducts of DNA replication, oxidative metabolism, ionizing radiation, and antigen receptor diversification reactions in lymphocytes (Hoeijmakers, 2009; Lieber, 2010; Nussenzweig and Nussenzweig, 2010). Joining of paired DNA breaks on disparate chromosomes leads to translocations, while joining of paired intrachromosomal breaks produces deletions that result in loss of genetic information. Translocations and deletions are commonly observed in cancer, where they are often recurrent and contribute to malignant transformation (Futreal et al., 2004).

HO, I-SceI, and zinc-finger nucleases that produce unique DSBs in yeast and mammalian genomes have been used to explore the biology of chromosome translocations. However, much less is known about the role of DNA repair factors in protecting cells against intrachromosomal deletions. In the absence of a sister chromatid, DSBs are repaired by either C-NHEJ or A-NHEJ. The C-NHEJ pathway requires DNA ligase IV, XRCC4, Ku70, and Ku80, and is necessary for efficient repair of intrachromosomal DSBs as evidenced by reduced CSR when C-NHEJ is impaired (Boboila et al., 2010a; Boboila et al., 2010b). Contrary to its role in promoting intrachromosomal DSB repair, the C-NHEJ pathway inhibits chromosome translocations, which often harbor microhomologies at the translocation breakpoint indicative of joining by the A-NHEJ pathway (reviewed in Kass and Jasin, 2010, and Zhang et al., 2010; Ramiro et al., 2006) To study the role of distance and DNA damage response factors in repair of tandem intrachromosomal DSBs in mammalian cells, we compared joining between I-SceI-induced DSBs on chromosome 12 spaced by 1.2 kb, 96 kb, and 27 Mb. Our analysis reveals that DSBs 1.2 kb or 96 kb apart are more likely to join than those separated by 27 Mb. Indeed, when DSBs are separated by 27 Mb on chromosome 12 the rate of paired end joining in *cis* is similar to transchromosomal joining between *IgH* and *c-myc* on chromosome 15.

53BP1 facilitates end joining in *cis* (Bothmer et al., 2010); however, this effect is limited to DSBs separated by 96 kb, as loss of 53BP1 does not reduce the joining frequency of proximal, very distal, or transchromosomal DSBs. The selective effect of 53BP1 on joining paired breaks separated by 96 kb suggests a role for DNA damage factors that spread along the chromosome in response to DSBs in an H2AX/RNF8-dependent manner (Bekker-Jensen et al., 2006; Savic et al., 2009). Indeed, the extent of γ-H2AX spreading from an I-SceI-induced DSBs at the IgH locus is confined to ~1 Mb surrounding the break (Figure S1I).

The new results are consistent with the finding that 53BP1 allows for a higher probability of interactions between DNA elements 28–172 kb apart during rearrangements of the TCRα locus (Difilippantonio et al., 2008). Since DSBs produced during CSR are separated by 60–200 kb, our findings support a model in which 53BP1 and possibly other focus forming factors promote the synapsis of DSBs if they fall within the range of spread of the H2AX/RNF8-dependent DNA damage response. Interestingly, loss of 53BP1 does not affect recombination efficiency mediated by Cre/loxP, which is independent of the DNA damage response (Bothmer et al., 2010; Guo et al., 1997). This indicates that indeed 53BP1 acts downstream of a DSB, mediating synapsis of broken ends as part of the DNA damage response.

In addition to forming repair foci at DNA ends 53BP1 also protects DNA ends from resection and thereby favors repair by C-NHEJ while preventing A-NHEJ (a pathway with extensive processing and microhomology) and HR (Bothmer et al., 2010; Bunting et al., 2010). This may be particularly important during CSR in lymphocytes because switch regions are highly repetitive. Since 53BP1 protects ends from resection, its absence would favor microhomology-mediated intraswitch joining as opposed to productive switch recombination between different switch regions (Bothmer et al., 2010). However, end protection is not sufficient to explain the effects of 53BP1 on CSR since H2AX deficiency promotes extensive end resection (Figure 4B) and yet produces a milder CSR defect (Reina-San-Martin

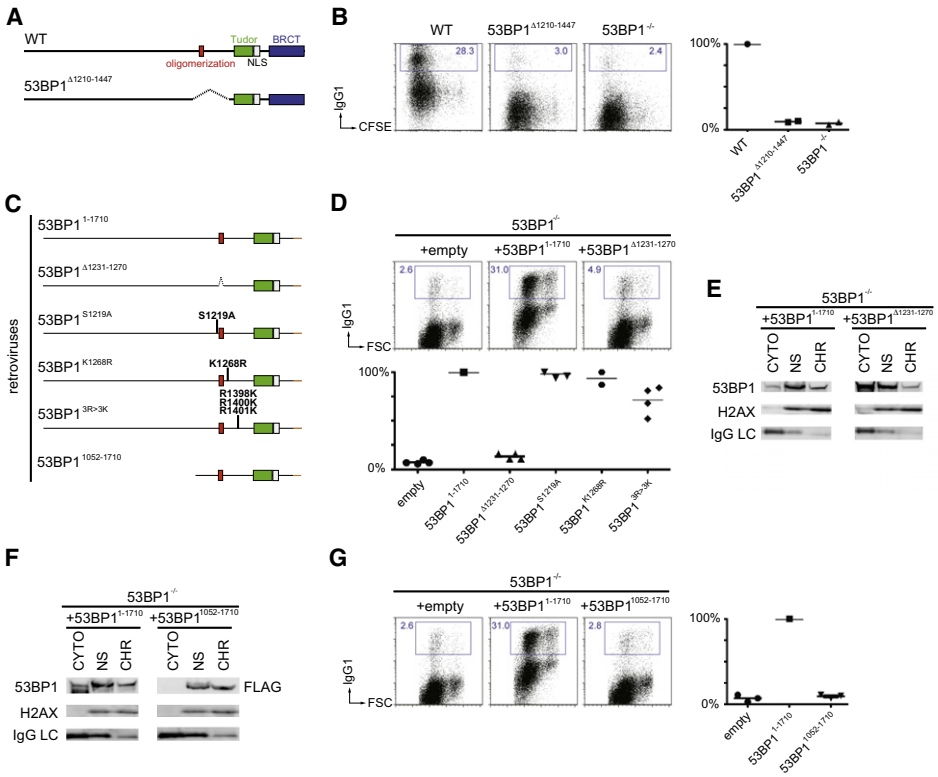

Figure 5. The Oligomerization Domain of 53BP1 in Chromatin Association and CSR

(A) Schematic representation of WT 53BP1 (top) and 53BP1 lacking amino acids 1210–1447 (bottom).

(B) As in Figure 2C for WT, 53BP1$^{\Delta 1210–1447}$, and 53BP1$^{-/-}$ B cells.

(C) Diagram of 53BP1 retroviral constructs with the indicated mutations and deletions.

(D) As in Figure 2C after infection of 53BP1$^{-/-}$ B cells with empty retrovirus, or retrovirus expressing 53BP1$^{1–1710}$, or the oligomerization mutant 53BP1$^{\Delta 1231–1270}$, or the other mutants listed in (C).

(E) Western blots of fractionated 53BP1$^{-/-}$ B cells stimulated and infected with 53BP1$^{1–1710}$ or 53BP1$^{\Delta 1231–1270}$.

(F) Western blots of fractionated 53BP1$^{-/-}$ B cells stimulated and infected with 53BP1$^{1–1710}$ or 53BP1$^{1052–1710}$.

(G) As in Figure 2C after infection of 53BP1$^{-/-}$ B cells with empty retrovirus, or retroviruses expressing 53BP1$^{1–1710}$ or the N-terminal deleted mutant 53BP1$^{1052–1710}$.

See also Figure S4.

et al., 2003). Of note, all joining experiments were performed in the absence of AID, and we cannot exclude the possibility that AID, in addition to 53BP1, influences the repair pathway choice.

The way in which 53BP1 mediates end protection and facilitates joining was investigated by analyzing the contribution of the structural domains of 53BP1 to DNA end protection and class switching in B lymphocytes. Human 53BP1 binds to the histone mark H4K20^{me2} via its tudor domain, and mutation of amino acid D1521 in the tudor domain abrogates 53BP1's ability to form DNA damage foci in response to IR (Botuyan et al., 2006; Huyen et al., 2004). We find that 53BP1 is chromatin associated even in the absence of DNA damage or H2AX, which is consistent with previous reports showing that H4K20^{me2} is a constitutive chromatin modification (Botuyan et al., 2006; Sanders et al., 2004) and that 53BP1 chromatin association is RNF8 independent (Santos et al., 2010). These studies suggest that even in the context of undamaged chromatin, this modification is accessible to 53BP1. Furthermore, a knockin mutant of the tudor domain (53BP1^{DR}) that fails to form foci in response to DNA damage also fails to associate with chromatin in nonirradiated cells. Therefore, an intact tudor domain is required for both constitutive binding to chromatin and DNA damage-induced focus formation. As predicted from its inability to bind chromatin or form DNA damage foci, 53BP1^{DR} was unable to protect DNA ends from resection or to support CSR.

The absence of 53BP1's oligomerization domain and deficiency in H2AX both impair the formation of stable DNA damage foci (Celeste et al., 2003; Fernandez-Capetillo et al., 2002; Ward et al., 2003; Yuan and Chen, 2010). In contrast, we find that neither the oligomerization domain of 53BP1 nor H2AX is required for 53BP1 binding to chromatin. However, DNA end protection and CSR are impaired in the absence of either. Thus, the ability to bind constitutively to chromatin appears to be necessary but not sufficient for end protection or CSR. Consistent with this idea, a fragment of 53BP1, which binds chromatin and forms DNA damage-inducible foci (53BP1$^{1052–1710}$), is unable to support either end protection or CSR. Interestingly, and unlike 53BP1, H2AX deficiency does not rescue the

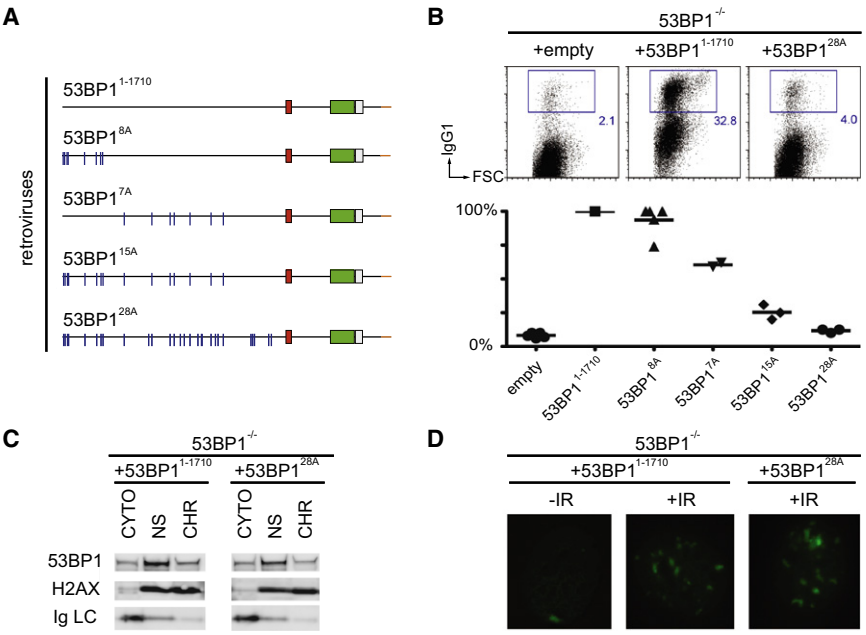

Figure 6. N-Terminal Phosphorylation of 53BP1 in DNA Damage and CSR

(A) Diagram of 53BP1 retroviral constructs with the indicated mutations.

(B) As in Figure 2C after infection of 53BP1$^{-/-}$ B cells with empty retrovirus, or retroviruses expressing 53BP1$^{1-1710}$, or the N-terminal mutant 53BP1^{28A}, or the other mutants listed in (A).

(C) Western blots of fractionated 53BP1$^{-/-}$ B cells stimulated and infected with 53BP1$^{1-1710}$ or 53BP1^{28A}.

(D) 53BP1 IRIF in 53BP1$^{-/-}$ MEFs reconstituted with 53BP1$^{1-1710}$ and 53BP1^{28A} after 10 Gy.

See also Figure S5.

formation of radial fusions observed in PARP inhibitor treated Brca1 mutant B cells (Figure 4C). Although deficiency in both H2AX and 53BP1 leads to increased end resection (Bothmer et al., 2010; Bunting et al., 2010; Helmink et al., 2011; Zha et al., 2011), H2AX—in contrast to 53BP1—probably plays additional roles in HR and NHEJ that may be essential in Brca1-deficient cells. Similar to H2AX, RNF8 and RNF168 are required for stable 53BP1 focus formation upon IR (Doil et al., 2009; Huen et al., 2007; Kolas et al., 2007; Mailand et al., 2007; Stewart et al., 2009; Yuan and Chen, 2010). In this context, it will be interesting to test the effect of RNF8/RNF168 deficiency on PARP inhibitor-induced chromosome abnormalities in Brca1$^{\Delta 11/\Delta 11}$ cells, as these ubiquitin ligases lie downstream of H2AX and upstream of 53BP1.

Our analysis of tandem BRCT domain-mutant B cells (53BP1$^{\Delta BRCT}$) showed that the C terminus is dispensable for both CSR and the protection of ends from processing, which suggests a role for the N terminus in these processes. The N terminus of 53BP1 lacks known structural domains but contains S/T-Q consensus target sites for ATM phosphorylation that are implicated in promoting the resolution of γ-H2AX foci upon IR (DiTullio et al., 2002; Morales et al., 2003; Ward et al., 2006). We find that the putative ATM phosphorylation sites are also required to prevent DNA resection and to support CSR, suggesting that N-terminally phosphorylated 53BP1 may recruit additional factors to regulate DNA repair. In summary (Figure 7B), out of all the 53BP1 functional domains tested, the ability to protect DNA ends from resection is the only parameter that correlates with CSR. Chromatin association, focus formation, oligomerization, and intact N-terminal ATM phosporylation sites are all essential but by themselves not sufficient to prevent DNA end processing or to support CSR. Therefore, end protection and CSR may not simply be mediated by direct physical association of 53BP1 with DNA ends but appear to require the assembly of a complex composed of H2AX, 53BP1, and possibly additional yet-to-be defined proteins.

EXPERIMENTAL PROCEDURES

Mice

IgH$^{I\text{-}1k/+}$, IgH$^{I\text{-}27M/+}$, 53BP1$^{\Delta BRCT/+}$, 53BP1$^{DR/+}$, and 53BP1$^{\Delta 1210\text{–}1447/+}$ mice were generated by homologous recombination in C57BL/6 albino embryonic stem cells (ESCs). Details of the targeting vectors, screening by Southern blot, and genotyping PCR are provided in the legends to Figures S1–S4. IgH$^{I\text{-}96k/+}$ (Bothmer et al., 2010), IgH$^{I/+}$ and Myc$^{I/+}$ (Robbiani et al., 2008), AID$^{-/-}$ (Muramatsu et al., 2000), 53BP1$^{-/-}$ (Ward et al., 2004), H2AX$^{-/-}$ (Celeste et al., 2002), Brca1$^{lox/lox}$ (Xu et al., 1999), Brca1$^{\Delta 11/\Delta 11}$ (Xu et al., 2001), and CD19^{cre} mice (Rickert et al., 1997) were previously described. Unless otherwise indicated, experiments were performed with mice homozygous for the indicated alleles. All experiments were performed in accordance with protocols approved by the Rockefeller University and National Institutes of Health (NIH) Institutional Animal Care and Use Committee.

Joining and Resection Analysis

The assay was performed as previously described (Bothmer et al., 2010). For details, see the Supplemental Experimental Procedures.

B Cell Cultures and Retroviral Infection

Resting B lymphocytes were isolated and stimulated for CSR as previously described (Robbiani et al., 2008). For analysis of radial structures, the PARP inhibitor KU58948 (1 μM) was added 16 hr before, and Colcemid (100 ng/ml, Roche) 1 hr before preparation of metaphase spreads (Bunting et al., 2010). For infection experiments, retroviral supernatants were prepared and administered as previously described (Robbiani et al., 2008). B cells were analyzed at 96 hr from the beginning of their culture.

Retroviruses

pMX-IRES-GFP based retroviruses encoding for I-SceI and catalytic mutant I-SceI* were previously described (Robbiani et al., 2008). Coding sequences of the human 53BP1 mutants were cloned into a modified pMX plasmid with deleted IRES-GFP (courtesy of Silvia Boscardin) to allow for proper packaging of this large protein. Therefore, in each experiment infection efficiency was monitored by western blot (see Figures S4–S6). 53BP1^{8A} encoded for the following alanine substitutions: S6A, S13A, S25A, S29A, S105A, S166A, S176A, and S178A. 53BP1^{7A} encoded for T302A, S452A, S523A, S543A, S625A, S784A, and S892A. 53BP1^{15A} encoded for the same alanine substitutions as in both 53BP1^{8A} and 53BP1^{7A}. In addition to these, 53BP1^{28A} also had S437A, S580A, S674A, T696A, S698A, S831A, T855A, S1068A, S1086A, S1104A, S1148A, T1171A, and S1219A. Unless otherwise noted, mutants bore a C-terminal HA-FLAG tag (in orange in Figures 5C and 6A and Figure S6).

A

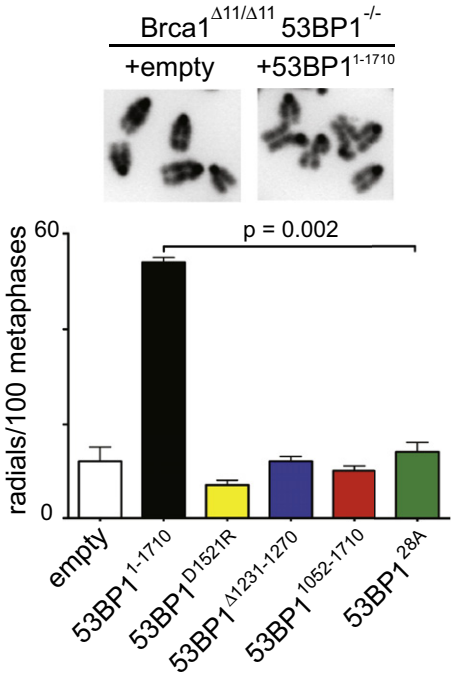

B

Domains of 53BP1	IRIF	Chromatin binding	CSR	Resection
BRCT	D	D	D	D
Tudor (D1518/D1521)	R	R	R	R
Oligomerization	R	D	R	R
N-terminal Phosphorylations	D	D	R	R

D = dispensable R = required

Figure 7. Domains of 53BP1 Required for Preventing DNA End Resection

(A) Brca1$^{\Delta11/\Delta11}$53BP1$^{-/-}$ B cells reconstituted with 53BP1 mutant retroviruses. Top: Examples of normal metaphases (+empty) or metaphases containing radial chromosome structures (+53BP1$^{1-1710}$). Bottom: Histogram quantitating the number of radial structures upon infection with the indicated retroviruses. Error bars indicate standard error of the mean. Two independent experiments.

(B) Table summarizing which functional domains of 53BP1 are required (R) or dispensable (D) for IRIF, chromatin binding, CSR, and protection of DNA ends from resection.

See also Figure S6.

Cell Fractionation and Western Blot

The cytoplasmic fraction from 5 Mio purified mutant splenic B cells (treated or not with 10 Gy IR and allowed 90 min recovery) was separated from the nuclei with the ProteoJET Cytoplasmic and Nuclear Protein Extraction Kit (Fermentas) according to the manufacturer's instructions. To separate nuclear-soluble and chromatin fractions, the manufacturer's nuclei lysis buffer was supplemented with the provided Nuclei Lysis reagent and with 30 mM EDTA, 2 mM EGTA, and 10 mM dithiothreitol. The nuclear extract was centrifuged at 1700 g for 20 min at 4°C; the supernatant was saved at −80°C as the "nuclear-soluble fraction," and the chromatin pellet was washed twice in 250 μl of 3 mM EDTA, 0.2 mM EGTA, 1 mM dithiothreitol, and protease inhibitors (Roche). Chromatin was resuspended in 30 μl of 10 mM HEPES, 10 mM KCl, 1 mM $MgCl_2$, 10% glycerol, 1 mM $CaCl_2$, 1 mM EDTA, 1× protease inhibitors (Roche), and 5 U micrococcal nuclease (New England Biolabs) and then incubated for 45 min at 37°C. The reaction was stopped by the addition of EGTA to 1 mM, and the digested pellet was stored at −80°C as the "chromatin-bound fraction." For retroviral reconstitution experiments, splenocytes were stimulated and fractionated on day 4. Expression of wild-type and mutant 53BP1 proteins was detected with antisera to 53BP1 (Bethyl), 53BP1 phosphorylated on Serine 25 (Bethyl), FLAG (SIGMA), or HA (Abcam) as indicated. Controls for DNA damage, cell fractionation, and loading were with antibodies to γ-H2AX (Millipore), H2AX (Bethyl), H4K20^{me1} (Abcam), IgG LC (Jackson Immunoresearch Laboratories), tubulin (Abcam), or actin (SIGMA).

Flow Cytometry

For fluorescence-activated cell sorting (FACS) analysis, spleen cell suspensions or cultures were stained with fluorochrome-conjugated anti-CD19, anti-CD3, anti-IgM, anti-IgD, and anti-IgG1 antibodies (PharMingen). Labeling for cell division was at 37°C for 10 min in 5 μM carboxyfluorescein succinimidyl esther (CFSE). Samples were acquired on a FACSCalibur instrument (Becton Dickinson) and analyzed with FlowJo software (Tree Star).

Ionizing Radiation Induced Foci and Laser Microirradiation

For IRIF, MEFs were grown overnight on glass coverslips in 30 mm culture dishes, then exposed to 5 Gy (53BP1 mutant MEFs) or 10 Gy (53BP1$^{-/-}$ MEFs reconstituted with mutant retroviruses) ionizing radiation and allowed to recover for 90 min. Cells were then fixed with 4% paraformaldehyde, followed by 0.5% Triton X-100 permeabilzation and processed for immunofluorescent staining at the indicated times after exposure. Images were acquired with an LSM 510 META microscope (Zeiss) or with DeltaVision (Applied Precision). For laser microirradiation, MEFs were grown in dye-free media. The DNA binding dye Hoechst 33258 was added at 10 mg/ml and incubated for 30 min at 37°C. After laser treatment, cells were allowed to recover for 30 min or 4 hr at 37°C and were subsequently fixed and processed for immunofluorescent staining as above. Primary antibodies used for immunofluorescence were rabbit anti-53BP1 (Novus Biologicals), mouse anti-γ-H2AX (Upstate Biotechnology), and mouse anti-FLAG-M2 (SIGMA). Secondary antibodies were Alexa568- and Alexa488-conjugated (Molecular Probes). DNA was counterstained with 4',6-diamidino-2-phenylindole (DAPI).

SUPPLEMENTAL INFORMATION

Supplemental Information includes Supplemental Experimental Procedures and six figures and can be found with this article online at doi:10.1016/j.molcel.2011.03.019.

ACKNOWLEDGMENTS

All members of the Nussenzweig labs for discussions. Thanos Halazonetis for wild type human 53BP1 plasmid and Philip Carpenter for plasmid with 53BP1 alanine substitutions. The Rockefeller University Gene Targeting Facility for the generation of mutant mice. The work was supported in part by a Fondazione Ettore e Valeria Rossi grant to D.F.R., by a NIH grant to M.C.N (AI037526), and a Department of Defense grant to A.N. (BC102335). A.N. and S.B. were supported by the Intramural Research Program of the NIH, the National Cancer Institute, and the Center for Cancer Research and I.A.K by NIH Medical Scientist Training Program grant GM07739. A.B. is a Predoctoral Fellow of the Cancer Research Institute, N.F. is and D.F.R. was a Fellow of the Leukemia and Lymphoma Society, M.D.V. is a Fellow of the American-Italian Cancer Foundation, and M.C.N. is a Howard Hughes Medical Institute Investigator.

Received: November 24, 2010
Revised: February 8, 2011
Accepted: March 28, 2011
Published: May 5, 2011

REFERENCES

Adams, M.M., and Carpenter, P.B. (2006). Tying the loose ends together in DNA double strand break repair with 53BP1. Cell Div. *1*, 19.

Anderson, L., Henderson, C., and Adachi, Y. (2001). Phosphorylation and rapid relocalization of 53BP1 to nuclear foci upon DNA damage. Mol. Cell. Biol. *21*, 1719–1729.

Bekker-Jensen, S., Lukas, C., Kitagawa, R., Melander, F., Kastan, M.B., Bartek, J., and Lukas, J. (2006). Spatial organization of the mammalian genome surveillance machinery in response to DNA strand breaks. J. Cell Biol. *173*, 195–206.

Boboila, C., Jankovic, M., Yan, C.T., Wang, J.H., Wesemann, D.R., Zhang, T., Fazeli, A., Feldman, L., Nussenzweig, A., Nussenzweig, M., and Alt, F.W. (2010a). Alternative end-joining catalyzes robust IgH locus deletions and translocations in the combined absence of ligase 4 and Ku70. Proc. Natl. Acad. Sci. USA *107*, 3034–3039.

Boboila, C., Yan, C., Wesemann, D.R., Jankovic, M., Wang, J.H., Manis, J., Nussenzweig, A., Nussenzweig, M., and Alt, F.W. (2010b). Alternative end-joining catalyzes class switch recombination in the absence of both Ku70 and DNA ligase 4. J. Exp. Med. *207*, 417–427.

Boisvert, F.M., Rhie, A., Richard, S., and Doherty, A.J. (2005). The GAR motif of 53BP1 is arginine methylated by PRMT1 and is necessary for 53BP1 DNA binding activity. Cell Cycle *4*, 1834–1841.

Bothmer, A., Robbiani, D.F., Feldhahn, N., Gazumyan, A., Nussenzweig, A., and Nussenzweig, M.C. (2010). 53BP1 regulates DNA resection and the choice between classical and alternative end joining during class switch recombination. J. Exp. Med. *207*, 855–865.

Botuyan, M.V., Lee, J., Ward, I.M., Kim, J.E., Thompson, J.R., Chen, J., and Mer, G. (2006). Structural basis for the methylation state-specific recognition of histone H4-K20 by 53BP1 and Crb2 in DNA repair. Cell *127*, 1361–1373.

Bunting, S.F., Callén, E., Wong, N., Chen, H.T., Polato, F., Gunn, A., Bothmer, A., Feldhahn, N., Fernandez-Capetillo, O., Cao, L., et al. (2010). 53BP1 inhibits homologous recombination in Brca1-deficient cells by blocking resection of DNA breaks. Cell *141*, 243–254.

Celeste, A., Petersen, S., Romanienko, P.J., Fernandez-Capetillo, O., Chen, H.T., Sedelnikova, O.A., Reina-San-Martin, B., Coppola, V., Meffre, E., Difilippantonio, M.J., et al. (2002). Genomic instability in mice lacking histone H2AX. Science *296*, 922–927.

Celeste, A., Fernandez-Capetillo, O., Kruhlak, M.J., Pilch, D.R., Staudt, D.W., Lee, A., Bonner, R.F., Bonner, W.M., and Nussenzweig, A. (2003). Histone H2AX phosphorylation is dispensable for the initial recognition of DNA breaks. Nat. Cell Biol. *5*, 675–679.

Difilippantonio, S., Gapud, E., Wong, N., Huang, C.Y., Mahowald, G., Chen, H.T., Kruhlak, M.J., Callen, E., Livak, F., Nussenzweig, M.C., et al. (2008). 53BP1 facilitates long-range DNA end-joining during V(D)J recombination. Nature *456*, 529–533.

Dimitrova, N., Chen, Y.C., Spector, D.L., and de Lange, T. (2008). 53BP1 promotes non-homologous end joining of telomeres by increasing chromatin mobility. Nature *456*, 524–528.

DiTullio, R.A., Jr., Mochan, T.A., Venere, M., Bartkova, J., Sehested, M., Bartek, J., and Halazonetis, T.D. (2002). 53BP1 functions in an ATM-dependent checkpoint pathway that is constitutively activated in human cancer. Nat. Cell Biol. *4*, 998–1002.

Doil, C., Mailand, N., Bekker-Jensen, S., Menard, P., Larsen, D.H., Pepperkok, R., Ellenberg, J., Panier, S., Durocher, D., Bartek, J., et al. (2009). RNF168 binds and amplifies ubiquitin conjugates on damaged chromosomes to allow accumulation of repair proteins. Cell *136*, 435–446.

Fernandez-Capetillo, O., Chen, H.T., Celeste, A., Ward, I., Romanienko, P.J., Morales, J.C., Naka, K., Xia, Z., Camerini-Otero, R.D., Motoyama, N., et al. (2002). DNA damage-induced G2-M checkpoint activation by histone H2AX and 53BP1. Nat. Cell Biol. *4*, 993–997.

Futreal, P.A., Coin, L., Marshall, M., Down, T., Hubbard, T., Wooster, R., Rahman, N., and Stratton, M.R. (2004). A census of human cancer genes. Nat. Rev. Cancer *4*, 177–183.

Guo, F., Gopaul, D.N., and van Duyne, G.D. (1997). Structure of Cre recombinase complexed with DNA in a site-specific recombination synapse. Nature *389*, 40–46.

Helmink, B.A., Tubbs, A.T., Dorsett, Y., Bednarski, J.J., Walker, L.M., Feng, Z., Sharma, G.G., McKinnon, P.J., Zhang, J., Bassing, C.H., and Sleckman, B.P. (2011). H2AX prevents CtIP-mediated DNA end resection and aberrant repair in G1-phase lymphocytes. Nature *469*, 245–249.

Hoeijmakers, J.H. (2009). DNA damage, aging, and cancer. N. Engl. J. Med. *361*, 1475–1485.

Huen, M.S., Grant, R., Manke, I., Minn, K., Yu, X., Yaffe, M.B., and Chen, J. (2007). RNF8 transduces the DNA-damage signal via histone ubiquitylation and checkpoint protein assembly. Cell *131*, 901–914.

Huen, M.S., Huang, J., Leung, J.W., Sy, S.M., Leung, K.M., Ching, Y.P., Tsao, S.W., and Chen, J. (2010). Regulation of chromatin architecture by the PWWP domain-containing DNA damage-responsive factor EXPAND1/MUM1. Mol. Cell *37*, 854–864.

Huyen, Y., Zgheib, O., Ditullio, R.A., Jr., Gorgoulis, V.G., Zacharatos, P., Petty, T.J., Sheston, E.A., Mellert, H.S., Stavridi, E.S., and Halazonetis, T.D. (2004). Methylated lysine 79 of histone H3 targets 53BP1 to DNA double-strand breaks. Nature *432*, 406–411.

Iwabuchi, K., Basu, B.P., Kysela, B., Kurihara, T., Shibata, M., Guan, D., Cao, Y., Hamada, T., Imamura, K., Jeggo, P.A., et al. (2003). Potential role for 53BP1 in DNA end-joining repair through direct interaction with DNA. J. Biol. Chem. *278*, 36487–36495.

Kass, E.M., and Jasin, M. (2010). Collaboration and competition between DNA double-strand break repair pathways. FEBS Lett. *584*, 3703–3708.

Kolas, N.K., Chapman, J.R., Nakada, S., Ylanko, J., Chahwan, R., Sweeney, F.D., Panier, S., Mendez, M., Wildenhain, J., Thomson, T.M., et al. (2007). Orchestration of the DNA-damage response by the RNF8 ubiquitin ligase. Science *318*, 1637–1640.

Lee, H., Kwak, H.J., Cho, I.T., Park, S.H., and Lee, C.H. (2009). S1219 residue of 53BP1 is phosphorylated by ATM kinase upon DNA damage and required for proper execution of DNA damage response. Biochem. Biophys. Res. Commun. *378*, 32–36.

Lieber, M.R. (2010). The mechanism of double-strand DNA break repair by the nonhomologous DNA end-joining pathway. Annu. Rev. Biochem. *79*, 181–211.

Mailand, N., Bekker-Jensen, S., Faustrup, H., Melander, F., Bartek, J., Lukas, C., and Lukas, J. (2007). RNF8 ubiquitylates histones at DNA double-strand breaks and promotes assembly of repair proteins. Cell *131*, 887–900.

Manis, J.P., Morales, J.C., Xia, Z., Kutok, J.L., Alt, F.W., and Carpenter, P.B. (2004). 53BP1 links DNA damage-response pathways to immunoglobulin heavy chain class-switch recombination. Nat. Immunol. *5*, 481–487.

Morales, J.C., Xia, Z., Lu, T., Aldrich, M.B., Wang, B., Rosales, C., Kellems, R.E., Hittelman, W.N., Elledge, S.J., and Carpenter, P.B. (2003). Role for the BRCA1 C-terminal repeats (BRCT) protein 53BP1 in maintaining genomic stability. J. Biol. Chem. *278*, 14971–14977.

Muramatsu, M., Kinoshita, K., Fagarasan, S., Yamada, S., Shinkai, Y., and Honjo, T. (2000). Class switch recombination and hypermutation require activation-induced cytidine deaminase (AID), a potential RNA editing enzyme. Cell *102*, 553–563.

Nussenzweig, A., and Nussenzweig, M.C. (2010). Origin of chromosomal translocations in lymphoid cancer. Cell *141*, 27–38.

Ramiro, A.R., Jankovic, M., Callen, E., Difilippantonio, S., Chen, H.T., McBride, K.M., Eisenreich, T.R., Chen, J., Dickins, R.A., Lowe, S.W., et al. (2006). Role of genomic instability and p53 in AID-induced c-myc-Igh translocations. Nature *440*, 105–109.

Rappold, I., Iwabuchi, K., Date, T., and Chen, J. (2001). Tumor suppressor p53 binding protein 1 (53BP1) is involved in DNA damage-signaling pathways. J. Cell Biol. *153*, 613–620.

Reina-San-Martin, B., Difilippantonio, S., Hanitsch, L., Masilamani, R.F., Nussenzweig, A., and Nussenzweig, M.C. (2003). H2AX is required for recombination between immunoglobulin switch regions but not for intra-switch region recombination or somatic hypermutation. J. Exp. Med. *197*, 1767–1778.

Reina-San-Martin, B., Chen, J., Nussenzweig, A., and Nussenzweig, M.C. (2007). Enhanced intra-switch region recombination during immunoglobulin class switch recombination in 53BP1-/- B cells. Eur. J. Immunol. *37*, 235–239.

Rickert, R.C., Roes, J., and Rajewsky, K. (1997). B lymphocyte-specific, Cre-mediated mutagenesis in mice. Nucleic Acids Res. *25*, 1317–1318.

Robbiani, D.F., Bothmer, A., Callen, E., Reina-San-Martin, B., Dorsett, Y., Difilippantonio, S., Bolland, D.J., Chen, H.T., Corcoran, A.E., Nussenzweig, A., and Nussenzweig, M.C. (2008). AID is required for the chromosomal breaks in c-myc that lead to c-myc/IgH translocations. Cell *135*, 1028–1038.

Sanders, S.L., Portoso, M., Mata, J., Bähler, J., Allshire, R.C., and Kouzarides, T. (2004). Methylation of histone H4 lysine 20 controls recruitment of Crb2 to sites of DNA damage. Cell *119*, 603–614.

Santos, M.A., Huen, M.S., Jankovic, M., Chen, H.T., López-Contreras, A.J., Klein, I.A., Wong, N., Barbancho, J.L., Fernandez-Capetillo, O., Nussenzweig, M.C., et al. (2010). Class switching and meiotic defects in mice lacking the E3 ubiquitin ligase RNF8. J. Exp. Med. *207*, 973–981.

Savic, V., Yin, B., Maas, N.L., Bredemeyer, A.L., Carpenter, A.C., Helmink, B.A., Yang-Iott, K.S., Sleckman, B.P., and Bassing, C.H. (2009). Formation of dynamic gamma-H2AX domains along broken DNA strands is distinctly regulated by ATM and MDC1 and dependent upon H2AX densities in chromatin. Mol. Cell *34*, 298–310.

Schultz, L.B., Chehab, N.H., Malikzay, A., and Halazonetis, T.D. (2000). p53 binding protein 1 (53BP1) is an early participant in the cellular response to DNA double-strand breaks. J. Cell Biol. *151*, 1381–1390.

Stavnezer, J., Guikema, J.E., and Schrader, C.E. (2008). Mechanism and regulation of class switch recombination. Annu. Rev. Immunol. *26*, 261–292.

Stewart, G.S., Panier, S., Townsend, K., Al-Hakim, A.K., Kolas, N.K., Miller, E.S., Nakada, S., Ylanko, J., Olivarius, S., Mendez, M., et al. (2009). The RIDDLE syndrome protein mediates a ubiquitin-dependent signaling cascade at sites of DNA damage. Cell *136*, 420–434.

Ward, I.M., Minn, K., Jorda, K.G., and Chen, J. (2003). Accumulation of checkpoint protein 53BP1 at DNA breaks involves its binding to phosphorylated histone H2AX. J. Biol. Chem. *278*, 19579–19582.

Ward, I.M., Reina-San-Martin, B., Olaru, A., Minn, K., Tamada, K., Lau, J.S., Cascalho, M., Chen, L., Nussenzweig, A., Livak, F., et al. (2004). 53BP1 is required for class switch recombination. J. Cell Biol. *165*, 459–464.

Ward, I., Kim, J.E., Minn, K., Chini, C.C., Mer, G., and Chen, J. (2006). The tandem BRCT domain of 53BP1 is not required for its repair function. J. Biol. Chem. *281*, 38472–38477.

Watanabe, K., Iwabuchi, K., Sun, J., Tsuji, Y., Tani, T., Tokunaga, K., Date, T., Hashimoto, M., Yamaizumi, M., and Tateishi, S. (2009). RAD18 promotes DNA double-strand break repair during G1 phase through chromatin retention of 53BP1. Nucleic Acids Res. *37*, 2176–2193.

Xu, X., Wagner, K.U., Larson, D., Weaver, Z., Li, C., Ried, T., Hennighausen, L., Wynshaw-Boris, A., and Deng, C.X. (1999). Conditional mutation of Brca1 in mammary epithelial cells results in blunted ductal morphogenesis and tumour formation. Nat. Genet. *22*, 37–43.

Xu, X., Qiao, W., Linke, S.P., Cao, L., Li, W.M., Furth, P.A., Harris, C.C., and Deng, C.X. (2001). Genetic interactions between tumor suppressors Brca1 and p53 in apoptosis, cell cycle and tumorigenesis. Nat. Genet. *28*, 266–271.

Yuan, J., and Chen, J. (2010). MRE11-RAD50-NBS1 complex dictates DNA repair independent of H2AX. J. Biol. Chem. *285*, 1097–1104.

Zgheib, O., Pataky, K., Brugger, J., and Halazonetis, T.D. (2009). An oligomerized 53BP1 tudor domain suffices for recognition of DNA double-strand breaks. Mol. Cell. Biol. *29*, 1050–1058.

Zha, S., Guo, C., Boboila, C., Oksenych, V., Cheng, H.L., Zhang, Y., Wesemann, D.R., Yuen, G., Patel, H., Goff, P.H., et al. (2011). ATM damage response and XLF repair factor are functionally redundant in joining DNA breaks. Nature *469*, 250–254.

Zhang, Y., Gostissa, M., Hildebrand, D.G., Becker, M.S., Boboila, C., Chiarle, R., Lewis, S., and Alt, F.W. (2010). The role of mechanistic factors in promoting chromosomal translocations found in lymphoid and other cancers. Adv. Immunol. *106*, 93–133.